

Local EGOP for Continuous Index Learning

Alex Kokot¹ Anand Hemmady² Vydhourie Thiyageswaran¹ Marina Meila³

Abstract

We introduce the setting of continuous index learning, in which a function of many variables varies only along a small number of directions at each point. For efficient estimation, it is beneficial for a learning algorithm to adapt, near each point x , to the subspace that captures the local variability of the function f . We pose this task as kernel adaptation along a manifold with noise, and introduce Local EGOP learning, a recursive algorithm that utilizes the Expected Gradient Outer Product (EGOP) quadratic form as both a metric and inverse-covariance of our target distribution. We prove that Local EGOP learning adapts to the regularity of the function of interest, showing that under a supervised noisy manifold hypothesis, intrinsic dimensional learning rates are achieved for arbitrarily high-dimensional noise. Empirically, we compare our algorithm to the feature learning capabilities of deep learning. Additionally, we demonstrate improved regression quality compared to two-layer neural networks in the continuous single-index setting.

1. Problem and approach

In a variety of contexts, including speech, images, and molecular dynamics, high-dimensional data often lie near a non-linear but low-dimensional manifold. Motivated by this phenomenon, we formulate the *supervised noisy manifold hypothesis (SNMH)*, which posits that a target function $f(x)$ varies along, but not orthogonally to, such a manifold \mathcal{M} . We call the problem of estimating f *continuous index learning (CIL)*, analogous to the well-studied problem of *multi-index learning (MIL)*, which assumes that \mathcal{M} is a linear subspace.

Given observations (x_i, y_i) , $i \in [n]$, multi-index learning is the task of estimating a function $f(x) := \mathbb{E}[Y|X = x]$ that

¹Department of Statistics, University of Washington

²Department of Biostatistics, University of Washington ³School of Computer Science, University of Waterloo. Correspondence to: Alex Kokot <akokot@uw.edu>.

Preprint. February 10, 2026.

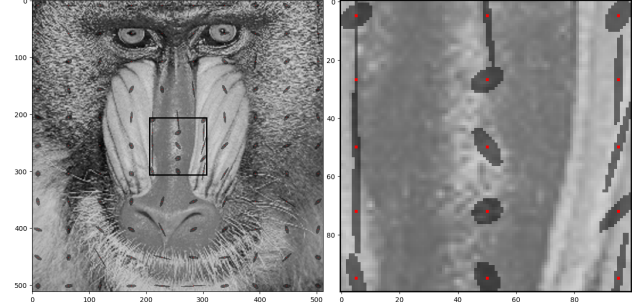


Figure 1. Localizations from Local EGOP Learning (Algorithm 1) centered at each of the highlighted points (in red) trained on a grayscale image of a mandrill [Bush \(2021\)](#). Here the inputs x are the pixel location and $f(x)$ is the grayscale value of the image. For visualization purposes the procedure was stopped early, and the 125 highest weight pixels are highlighted at each point. On the right the image is magnified to the highlighted region boxed-off on the left.

only depends on x through composition with a low-rank matrix V , i.e. $f(x) = g(Vx)$. In CIL, we allow V_x to be a continuously varying affine map, i.e. $f(x) = g(V_x x)$, and $\nabla V_x \eta = 0$ for all η such that $V_x(x+\eta) = V_x(x)$. Due to the SNMH, $f(x) = g(\pi(x))$ where $\pi(x) := \operatorname{argmin}_{q \in \mathcal{M}} \|q - x\|$ denotes the nearest point projection onto \mathcal{M} . For such data we call the space normal to \mathcal{M} , denoted $U_{\pi(x)}$, the *uninformative subspace*, as f does not vary along these directions. We refer to the tangent directions, denoted $V_x = U_{\pi(x)}^\perp$, as the *informative subspace*.

We approach estimating $f(x)$ via kernel smoothing, letting

$$\hat{f}(x) = \sum_i w_i Y_i, \text{ with } w_i \propto k_h(x, X_i) \quad (1)$$

for a kernel k and bandwidth h . For convenience, we use a Gaussian kernel for k , although modifications for the general setting are presented in Appendix B.1.4.

We propose that the k_h be *anisotropic*, emulating the local multi-index structure of f through the Mahalanobis metrization $k_h(x, X_i) = k(\|M^{1/2}(x - X_i)\|/\sqrt{2h})$. Specifically, if M can be selected to degenerate along the normal $U_{\pi(x)}$, then the weights w_i will decay primarily along the informative tangent direction V_x , leading to estimation rates scaling with the dimension d of the intrinsic manifold \mathcal{M} .

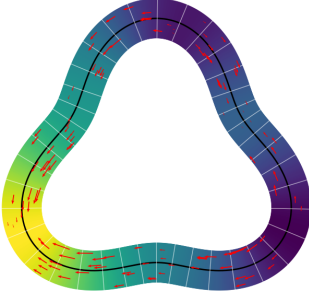


Figure 2. Supervised noisy manifold data in \mathbb{R}^2 . In a neighborhood about a closed curve we overlay a heatmap of a function invariant to normal displacement. The curve is displayed in black, the normal spaces are highlighted in white, and red gradients are displayed at randomly sampled points, with lengths proportionate to the gradient magnitude.

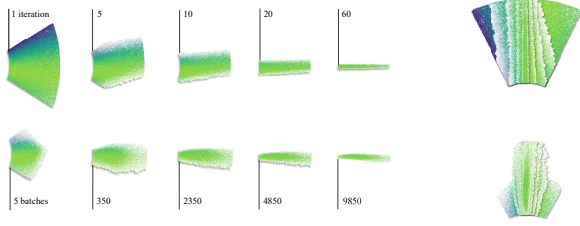
We then develop a recursive procedure we call *Local EGOP Learning*, which iteratively refines the metric M by pooling coarse differential information estimated from the observed data around a target point x^* , without a priori knowledge of the manifold \mathcal{M} .

Our method draws inspiration from recent works such as Radhakrishnan et al. (2022); Beaglehole et al. (2023); Radhakrishnan et al. (2025); Zhu et al. (2025); more background can be found in Section 2. Central in this line of research is the expected gradient outer product (EGOP), $\mathcal{L}(\mu) := \int \nabla f \nabla f^T d\mu$. Its empirical counterpart is the average gradient outer product (AGOP), $\hat{\mathcal{L}}(P_n) := \mathcal{L}_{\hat{f}}(P_n) := \frac{1}{n} \sum_{i=1}^n \nabla \hat{f}(x_i) \nabla \hat{f}^T(x_i)$, with P_n the empirical distribution, \hat{f} an estimator of f . In this paper, we focus on the problem of point estimation, where f is estimated at a specified query point x^* . Our key insight is to iteratively *localize* the EGOP (or AGOP) around the point of interest x^* . At a given iteration t , we set $w_i^{(t)} \propto k(\|\hat{M}_t^{1/2}(x^* - X_i)\|/\sqrt{2h_{t+1}})$, use \hat{f} given by (1), and compute

$$\hat{\mathcal{L}}_t := \hat{\mathcal{L}} \left(\sum_{i=1}^n w_i^{(t)} \delta_{x_i} \right) = \sum_{i=1}^n w_i^{(t)} \nabla \hat{f}(x_i) \nabla \hat{f}(x_i)^T.$$

That is, rather than averaging the gradient outer products over the full dataset, we *weigh* them with respect to the same kernel we utilize for regression. In the subsequent iteration, we update the metric \hat{M}_{t+1} using $\hat{\mathcal{L}}_t$, thus steering the kernel with this differential information. This recursion is at the core of Algorithm 1 described in Section 3,

In Section 4, we analyze this recurrence through its continuum counterparts, $\mu_{t+1} := N(x^*, h_{t+1} M_t^{-1})$, $M_t := \beta \mathcal{L}(\mu_t) + (1 - \beta) \mathcal{L}(\mu_{t-1})$. In Section 5, we numerically validate these results, and compare the performance of our proposed estimator to various neural network architectures, while Section 6 indicates avenues for future work. Our main contributions are:



(a) Localizations μ_i from Local EGOP (top) and neural network learning (bottom) and a deep neural network (bottom) localizations.

Figure 3. Local EGOP Learning and a deep transformer architecture applied to data sampled from an annulus. Labels are generated with no dependence on the radius in the parameterization, with these values overlaid as a heatmap. About the point $x^* = (1, 0)$, points are displayed with opacity $w \propto \exp(-d(x^*, x_i)^2)$, where $d(\cdot, \cdot)$ is the AGOP Mahalanobis distance (top) and transformer feature embedding (bottom). Both regions are displayed after progressively many iterations/training batches.

1. Introducing the setting of continuous index learning, generalizing multi-index learning to latent manifold structures.
2. Developing the Local EGOP Learning Algorithm and the localization of the EGOP.
3. Analyzing the recurrence and the resulting intrinsic dimensional learning rate of Local EGOP Learning under the SNMH (Sections 4.3 and 4.4).
4. Establishing a novel approach for the study of recursive kernel learning such as Radhakrishnan et al. (2022; 2025); Zhu et al. (2025).
5. Clarifying the role of the EGOP in the minimization of the mean squared error via a new functional framework.

2. Background and Related Work

Kernel methods are a powerful mechanism for studying machine learning algorithms. Many algorithms have leveraged the corresponding RKHS structure for efficient estimation of sufficiently regular functions (Wainwright, 2019), and functionals (Rao, 2014). Further, many popular learning algorithms, such as certain neural network architectures and random forests, have been shown to asymptotically correspond to carefully chosen kernels (Jacot et al., 2018; Scornet, 2016). Thus, the process by which investigators select kernels tailored to problems of interest, known as kernel engineering, is of central importance (Belkin et al., 2018). Beyond allowing for potential efficiency gains, kernel engineering closely emulates the feature learning properties of deep neural networks.

Some objectives of kernel engineering include the design of specialized kernels suited to particular data structures (Odone et al. (2005); Kondor & Jebara (2003); Joachims (1998); Chapelle et al. (1999); Barla et al. (2002); Vishwanathan et al. (2010), etc.), statistical principles (Genton (2001); Schölkopf et al. (1997); Osborne (2010), etc.), and problems of interest (Gong et al. (2024); Kokot & Luedtke (2025), etc.). In regression settings, a classical approach is local feature learning, in which kernels are augmented by differential information at points of interest (Schmid & Mohr (1997); Lowe (1999); Wallraven et al. (2003)). Earlier nonparametric methods developed a similar framework, with datasets being recursively partitioned to improve the quality of local fits (Heise, 1971; Breiman & Meisel, 1976; Friedman, 1979).

A modern incarnation of kernel engineering is *multi-index learning*, particularly in the case of neural networks (Mousavi-Hosseini et al. (2022); Boix-Adsera et al. (2023); Damian et al. (2023), etc.). This literature aims to show that the desirable properties of kernel engineering, such as data adaptivity and dimension reduction, are captured implicitly by certain machine learning models. Much work has been done in the *single-index* case, where the goal is to regress labels Y on features X when f depends on x solely through its evaluation in a fixed direction v , via the quantity $v^T x$. It has been shown that two-layer neural networks not only learn this dependence, but do so efficiently, leading to rapid increases in prediction quality (Bietti et al. (2022); Abbe et al. (2024); Lee et al. (2024), etc.). Recent results indicate that these same benefits carry over to the multi-index setting (Damian et al., 2023; Arnaboldi et al., 2024).

The SNMH feature structure is typical in manifold learning (Aamari & Levraud, 2018; Genovese et al., 2012; Kokot et al., 2025). It also appears under a different name (the “nonlinear single-variable model”) in the recent work (Wu & Maggioni, 2024), where the analysis is specialized to a 1-dimensional intrinsic manifold. They relate this problem to the more general settings of compositional learning (Juditsky et al. (2009); Shen et al. (2021), etc.) and non-linear dimension reduction (Yeh et al. (2008); Lee et al. (2013), etc.). In this literature, many recent methods propose similarly motivated optimization schemes that target related Poincaré inequalities (Bigoni et al., 2022; Verdière et al., 2025; Nouy & Pasco, 2025).

Our method bears a particularly strong resemblance to “kernel steering” as proposed in the image processing literature (Takeda et al., 2007; 2008). The EGOP has been motivated in many statistical applications (Samarov, 1993; Hristache et al., 2001; Xia et al., 2002; Trivedi et al., 2014; Yuan et al., 2023). A precursor in a supervised *noiseless* manifold setting is Aswani et al. (2011); in this paper, intrinsic rates are achieved with an *isotropic kernel* and sparse regression,

where the regression coefficients are penalized differently in the normal and tangent space to \mathcal{M} . Unlike our work and much of the literature, the method is extended to the regime where the number of regressors tends to infinity. The methods are not adaptive, an outer procedure must estimate the local dimension d .

Besides kernel steering, EGOP metrizations have appeared in many different literatures, with common goals being to accelerate learning tasks and learn efficient dimension reductions (Trivedi et al., 2014; Wu et al., 2010; Mukherjee et al., 2010).

3. The Local EGOP Algorithm

In this section, we introduce the Local EGOP Learning algorithm, detailed in Algorithm 1.

At iteration t , the algorithm uses the Gaussian kernel with Mahalanobis metric M_t (step 3) to estimate the local density μ_t about x^* . Using this weighting, \hat{f} and its gradients are computed (steps 5–7), which in turn are used to calculate the AGOP, L_t . This is then incorporated into the new metric $M_{t+1} = [\beta L_t + (1 - \beta)L_{t-1}]$, $\beta \in (0, 1)$. In practice, one might choose hyper-parameters β, T , as well as the schedule $\{h_t\}$ via cross-validation. For computational reasons, we normalize M_t by its trace (step 20) when applying the scaling factor h_{t+1} . This has little impact asymptotically, as the trace converges to the leading gradient eigenvalue of the EGOP, making this normalization effectively equivalent to a constant scaling. However, it serves a practical benefit by stabilizing initial iterates, setting the scale of the metric to the predefined rate $1/h_t$. Note that while the optimal number of iterations is dimension-dependent, as argued in Theorems 1 and 3, our algorithm incorporates a Leave-One-Out style validation loop (step 10) for adaptive stopping. Further theoretical motivation for the algorithm is presented in Section 4.3.

The time complexity of Algorithm 1 is $O(T((m+2)nD^2 + (m+1)D^3))$, with memory overhead $O(nD^2 + m^2D^2 + mD^3)$.

4. Theoretical analysis

We now study Algorithm 1 through its continuum t counterparts, described by $\mu_{t+1} := N(x^*, h_{t+1}M_t^{-1})$ and $M_t := \beta\mathcal{L}(\mu_t) + (1 - \beta)\mathcal{L}(\mu_{t-1})$. Setting $\Sigma_t := \Sigma(\mu_t) := \int(x - x^*)(x - x^*)^T d\mu_t$, this reduces to the matrix recurrence

$$\Sigma_{t+1} = h_{t+1}[\beta\mathcal{L}(\mu_t) + (1 - \beta)\mathcal{L}(\mu_{t-1})]^{-1}. \quad (2)$$

In Section 4.2 we propose a framework for the analysis of the resulting estimator. We introduce the EGOP form $W(\mu_t) := \text{tr}(\mathcal{L}(\mu_t)\Sigma(\mu_t))$, relating it to the bias of the M_t

Algorithm 1 Local EGOP Learning

Input: Data $\{(X_j, Y_j)\}_{j=1}^n$, target x^* , subsample size m , iterations T , bandwidths $\{h_t\}$, $\beta > 0$, scale $\alpha > 0$.

Output: Best estimate $\hat{f}(x^*)$.

Hyperparameters: $M_0 \leftarrow I/\alpha$.

```

1: bestMSE  $\leftarrow \infty$ ,  $\hat{f}_{\text{best}}(x) \leftarrow \emptyset$ 
2: for  $t = 0$  to  $T - 1$  do
3:    $\triangleright$  Compute weights at  $x^*$ 
4:    $w_i \propto \exp(-(x_i - x^*)^\top M_t(x_i - x^*))$ ,  $i = 1, \dots, n$ 
5:   Normalize  $w$ , subsample  $S \subset \{1, \dots, n\}$ ,  $|S| = m$  with probs  $w$ 
6:    $\triangleright$  Leave-One-Out Local regressions at each  $i \in S$ 
7:   for  $i \in S$  do
8:     Fit weighted local linear regression centered at  $x_i$  (weights from metric  $M_t$ ), excluding  $(x_i, y_i)$ 
9:     Obtain  $\nabla \hat{f}[i]$  and  $\hat{f}[i]$ 
10:    end for
11:     $\triangleright$  Aggregate statistics
12:     $L_t \leftarrow \sum_{i \in S} w_i \nabla \hat{f}[i] \nabla \hat{f}[i]^\top$ 
13:     $\widehat{\text{MSE}}_t \leftarrow \sum_{i \in S} w_i (y_i - \hat{f}[i])^2$ 
14:    if  $\widehat{\text{MSE}}_t < \text{bestMSE}$  then
15:      Estimate  $\hat{f}(x^*)$  via local regression centered at  $x^*$ 
16:       $\text{bestMSE} \leftarrow \widehat{\text{MSE}}_t$ ,  $\hat{f}_{\text{best}}(x^*) \leftarrow \hat{f}(x^*)$ 
17:    end if
18:     $\triangleright$  Metric update: set  $\beta = 1$  if  $i = 0$ ,  $\beta < 1$  otherwise
19:     $M_{t+1} \leftarrow (\beta L_t + (1 - \beta) L_{t-1})$ 
20:     $M_{t+1} \leftarrow M_{t+1} / [t_{t+1} \text{tr}(M_{t+1})]$ 
21:  end for
22: return  $\hat{f}_{\text{best}}(x)$ 

```

metrized kernel smoother via a Poincaré inequality. Building on this, in Section 4.3, we demonstrate how this recursive kernel adaptation can be naturally framed as a greedy MSE reduction strategy. In Section 4.4, our analysis yields an intrinsic learning rate for supervised noisy manifold data, and a significant efficiency gain otherwise.

4.1. Assumptions and Notation

We refer to the population distribution of our feature vectors $X \in \mathbb{R}^D$ as P , and its empirical distribution as P_n . We assume P has bounded C^1 density with respect to the Lebesgue measure on \mathbb{R}^D . When invoking the noisy manifold hypothesis, we denote by \mathcal{M} the smooth base manifold of dimension d , by π the nearest point projection onto the manifold, and by \mathcal{T}_x and \mathcal{N}_x the tangent and normal spaces $U_{\pi(x)}$ and V_x , respectively, at point $p := \pi(x) \in \mathcal{M}$. For π to be well-defined, we further assume that X lies within the reach of \mathcal{M} (Federer, 1959) almost surely. The labels Y are assumed to be of the form $Y_i = f(X_i) + \varepsilon_i$ for ε_i iid, mean zero, and finite 4th moment. We assume that $f \in C^4$

and is bounded with uniformly bounded derivatives. We reserve μ to refer to a localization or target distribution of data appropriately concentrated about the point of interest x^* . We denote by Σ the covariance of μ , and we enforce $\|\Sigma\| \leq \zeta < \infty$. We denote by $\langle \cdot, \cdot \rangle_F$ the Frobenius inner product. We assume $g = \nabla f(x^*) \neq 0$. We denote by k a second-order kernel that satisfies typical assumptions in the nonparametric statistics literature, as in, for example, (Tsybakov, 2009)[Chapter 1].

4.2. Bias Control via EGOP

In this section, we develop a theoretical framework for adaptive kernel learning. Define the empirical kernel estimator for predicting the value of f at x^* by

$$\hat{P}_{M_t}(f) := \frac{1}{\hat{C}_{M_t}} \frac{1}{n} \sum_{i=1}^n k(\|M_t^{1/2}[X_i - x^*]\|/\sqrt{2h_{t+1}}) Y_i,$$

$$\hat{C}_{M_t} := \frac{1}{n} \sum_{i=1}^n k(\|M_t^{1/2}[X_i - x^*]\|/\sqrt{2h_{t+1}}).$$

Its continuous counterpart is

$$P_{M_t}(f) := \frac{1}{C_{M_t}} \int k(\|M_t^{1/2}[y - x^*]\|/\sqrt{2h_{t+1}}) f(y) dP(y),$$

$$C_{M_t} := \int k(\|M_t^{1/2}[y - x^*]\|/\sqrt{2h_{t+1}}) dP(y).$$

The bandwidth h is suppressed in our notation as it will be pre-set at each iteration of our algorithm. To assess the quality of this predictor, we can measure its bias $\int (P_{M_t}(f) - f)^2 d\mu$ on a target distribution μ . When M and μ are chosen in tandem, the bias can be related to a Dirichlet form in terms of the EGOP. To make this explicit, we introduce the EGOP form

$$W(\mu) := \int \nabla f^\top \Sigma(\mu) \nabla f d\mu = \text{tr}(\mathcal{L}(\mu) \Sigma(\mu)). \quad (3)$$

Lemma 1 (Poincaré Inequality). *Let $M_t \succeq 0$, and set $\mu_{t+1} = N(0, h_{t+1} M_t^{-1})$. Then,*

$$\int (P_{M_t}(f) - f)^2 d\mu_{t+1} = O(W(\mu_{t+1})).$$

In the anisotropic metric M_t , the variation of f is given by $\mathcal{L}(\mu_{t+1})$, and the variance of x is given by $\Sigma(\mu_{t+1})$. If these matrices are close to low-rank and perpendicular, then the bias of the kernel estimator is controlled by $W(\mu_{t+1}) = \langle \mathcal{L}(\mu_{t+1}), \Sigma(\mu_{t+1}) \rangle_F$, and will be nearly 0. Of critical importance are the first and second moments of the target distribution μ , motivating our Gaussian convention, although Gaussianity is not essential to achieve the desired bound. We note that this general structure, of metrizing by the inverse covariance, appears in disparate

literatures, from classical local feature estimators (Schmid & Mohr, 1997), to VAEs (Chadebec & Allassonnière, 2022), and Langevin preconditioning (Cui et al., 2024).

We now seek to control the variance of the finite sample estimator \hat{P}_M of f at x^* .

Lemma 2 (Variance). *Let $M_t \succeq 0$, $\Sigma_{t+1} = h_{t+1}M_t^{-1}$. Then $\mathbb{E}[(\hat{P}_{M_t}(f) - P_{M_t}(f))^2] = O(1/(n\sqrt{\det \Sigma_{t+1}}))$.*

Combining these bounds yields our fundamental error rate.

Theorem 1 (Local MSE). *Let $M_t \succeq 0$, and set $\Sigma_{t+1} = h_{t+1}M_t^{-1}$, $\mu_{t+1} = N(x^*, \Sigma_{t+1})$. Then,*

$$\mathbb{E} \left[\int (\hat{P}_{M_t}(f) - f)^2 d\mu_{t+1} \right] = O \left(\frac{1}{n\sqrt{\det \Sigma_{t+1}}} + W(\mu_{t+1}) \right).$$

In particular, if $W(\mu_t) = O(h_t)$ and $\det \Sigma_t = O(h_t^q)$ then the asymptotic learning rate is

$$\mathbb{E} \left[\int (\hat{P}_{M_t}(f) - f)^2 d\mu_{t+1} \right] = O \left(n^{-\frac{1}{1+q/2}} \right).$$

4.3. Recursive Kernel Learning as Variance Minimization

We will now show how recursive kernel learning, combined with our basic kernel bounds, constitutes a greedy variance reduction strategy. Intuitively, the goal is to induce anisotropy in the kernel, stretching or steering it to include additional low-bias points that would otherwise be discarded with an isotropic metric. The inclusion of these additional high-quality points is exactly a reduction of variance, as including more data results in tighter concentration to the mean for a local averaging estimator.

We now make precise how one can arrive at this by leveraging Theorem 1. Ideally, as spelled out in this result, we would like to select μ_t such that $W(\mu_t) \rightarrow 0$, and that $\det \Sigma(\mu_t)$ is as large as possible. In other words, if we specify the rate $W(\mu_t) = \text{tr}[\mathcal{L}(\mu_t)\Sigma(\mu_t)] = h_t \rightarrow 0$, it would be optimal to select the largest possible region that achieves this bias, meaning we would like to select

$$\mu_t = \text{argmax}_{\text{tr}[\mathcal{L}(\mu_t)\Sigma(\mu_t)] \leq h_t} \log \det \Sigma(\mu_t).$$

This however cannot be solved, as we lack precise knowledge of the target function f . Moreover, $\text{tr}[\mathcal{L}(\mu_t)\Sigma(\mu_t)] \leq h_t$ presents a challenging feasible set, as it is posed over a space of probability distributions, thus making it non-Euclidean. Our Gaussian ansatz reduces the problem to optimizing a finite parameterization, though the optimization is non-convex.

This leads us to the following discretized relaxation of the problem. Set $\mu_0 = N(x^*, \alpha I)$, an isotropic initialization. If we compute the initial $\hat{\mathcal{L}}(\mu_0)$, we may hope that, as

long as μ_1 represents a sufficiently comparable distribution, $\hat{\mathcal{L}}(\mu_0) \approx \hat{\mathcal{L}}(\mu_1)$. Thus, we can compute

$$\Sigma_1 = \text{argmax}_{\text{tr}[\hat{\mathcal{L}}(\mu_0)\Sigma] \leq t_1} \log \det \Sigma = h_1 \hat{\mathcal{L}}(\mu_0)^{-1} / D.$$

This yields $\mu_1 = N(x^*, \Sigma_1)$, and the corresponding kernel estimator is metrized by $\Sigma_1^{-1} \propto \hat{\mathcal{L}}(\mu_0)$. Repeating this, we have a recursive kernel learning algorithm, as we summarize below.

Proposition 1 (Alternating Minimization). *Let $h_t \rightarrow 0$, fix Σ_0 , $\mu_t = N(x^*, \Sigma_t)$, $\hat{\mathcal{L}}_t := \hat{\mathcal{L}}(\mu_t)$, and construct $\hat{f} = \hat{P}_{\Sigma_t^{-1/2}}(f)$. Let Σ_t satisfy the recursive kernel recurrence $\Sigma_{t+1} = h_{t+1} \hat{\mathcal{L}}_t^{-1} / D$. Then, equivalently, optimizing over $\Sigma \succeq 0$,*

$$\begin{aligned} \Sigma_{t+1} &= \text{argmax}_{\text{tr}[\hat{\mathcal{L}}(\mu_t)\Sigma] \leq h_{t+1}} \log \det \Sigma & (4) \\ &= \text{argmin}_{\text{tr}[\hat{\mathcal{L}}(\mu_t)\Sigma] = h_{t+1}} \text{tr}(\hat{\mathcal{L}}(\mu_t)\Sigma) + \frac{1}{n\sqrt{\det \Sigma}}. \end{aligned}$$

We note that in Algorithm 1, we use local linear regression to better fit into the EGOP estimation loop, and we develop corresponding theory in Appendix C.

From this framework we have developed, it is clear that there are many possible schemes to optimize the bias-variance trade-off, and we discuss this in more detail in Section 6. We choose to focus on this alternating optimization because it strongly resembles algorithms present in the existing literature, and is simple to implement.

4.4. Bias-Variance trade-off – Convergence at intrinsic rate

In this section, we demonstrate concrete theoretical guarantees for estimation via Local EGOP Learning. For ease of presentation, in the main text we consider an iterative scheme in which an oracle EGOP is queried for a particular choice of covariance. In Appendix C we develop theory towards EGOP approximation, showing that anisotropic smoothing is compatible with recursive kernel learning under standard nonparametric estimation rates. For our experiments, we compute empirical AGOPs fit via the proposed iterative estimation procedure, leading to sharp estimation. See Appendix B for proofs of all following arguments.

4.4.1. TAYLOR EXPANSION

Up to this point, our prevailing perspective is that the target distributions μ matter up to their first and second moments, passing the optimization problem from the space of measures to the PSD cone, and facilitating a Gaussian relaxation. We close the loop to EGOP estimation by additionally Taylor expanding $\mathcal{L}(\mu)$ up to second order, reducing the proposed iteration scheme entirely to a recurrence in Σ .

Lemma 3 (Generic Taylor Expansion). *Let $\mu = N(x^*, \Sigma)$, $g = \nabla f(x^*)$, and $H = \nabla^2 f(x^*)$. Then there exist $T : \mathbb{R}^{D \times D} \rightarrow \mathbb{R}^D$, $R : \mathbb{R}^{D \times D} \rightarrow \mathbb{R}^{D \times D}$, $C_T \geq 0$, and $C_R \geq 0$ such that for any $A \succeq 0$, $\|T(A)\| \leq C_T \|A\|$, $\|R(A)\| \leq C_R \|A\|^2$, and*

$$\mathcal{L}(\mu) = gg^T + H\Sigma H + gT(\Sigma)^T + T(\Sigma)g^T + R(\Sigma).$$

Define $T_g(\Sigma) := gT(\Sigma)^T + T(\Sigma)g^T$. Our goal is to analyze

$$\begin{aligned} \Sigma_{t+1} &= h_{t+1}(\beta\mathcal{L}(\mu_t) + (1-\beta)\mathcal{L}(\mu_{t-1}))^{-1} \\ &= h_{t+1}(gg^T + \beta[H\Sigma_t H + T_g(\Sigma_t) + R(\Sigma_t)], \\ &\quad + (1-\beta)[H\Sigma_{t-1} H + T_g(\Sigma_{t-1}) + R(\Sigma_{t-1})])^{-1}. \end{aligned}$$

We initialize this recurrence with the isotropic choice $\Sigma_0 = \alpha I$, $\Sigma_1 = t_1\mathcal{L}(\mu_0)^{-1}$, $\Sigma_2 = t_1\mathcal{L}(\mu_1)^{-1}$, then apply the momentum β following this step.

4.4.2. FULL RANK HESSIAN

We begin our analysis with the generic setting, where H is full-rank. Here, the Taylor expansion of $\mathcal{L}(\mu)$ is dominated by a rank 1 matrix gg^T and a linear term $H\Sigma H$, which combine to yield a full rank matrix. We argue that $g^T\Sigma_t g = \Theta(h_t)$, while for $v \perp g$, $v^T\Sigma_t v = \Theta(\sqrt{h_t})$, thus achieving a second-order anisotropy.

Example 1 (Scalar Recurrence). Fix a schedule for $h_t \rightarrow 0$ such that h_{t+1}/h_t is larger than a fixed threshold. Consider the one dimensional recurrences

$$a_{t+1} = \frac{h_{t+1}}{\beta a_t + (1-\beta)a_{t-1}}, \quad (5)$$

$$b_{t+1} = \frac{h_{t+1}}{c + \beta b_t + (1-\beta)b_{t-1}}. \quad (6)$$

It is easy to see that $b_t = O(h_t)$, as if b_t decays at all, then we have $b_t = h_{t+1}/c + o(h_t)$. Assume that $a_t = \Theta(h_t^\zeta)$. By the recurrence relation, we then have $a_i = \Theta(h_i^{1-\zeta})$, and so these coincide at the second order anisotropy $\zeta = 1/2$. As our matrix recurrence is primarily given by a homogeneous part ($H\Sigma H$) plus a rank deficient constant part (gg^T), we argue in Appendix B that the b_t correspond well to the $g \times g$ block of Σ_t , and a_i to $g^\perp \times g^\perp$.

Example 2 (Momentum). We now take a moment to highlight the necessity of the momentum term $\beta \in (0, 1)$. Consider, again, the sequence a_t from Example 1, and suppose we set $\beta = 1$. For convenience, let us assume $\sqrt{h_{t+1}} = \sqrt{h_t}r$, an exact geometric schedule. We reparameterize, writing

$$a_{t+1} = \frac{h_{t+1}}{a_t} \iff a'_{t+1} = \frac{1}{a'_t}$$

for $a'_i := \frac{a_i}{\sqrt{r}t_i}$. Clearly, a'_t has no limit, as it oscillates about 1. In the corresponding matrix recurrence, the remainder

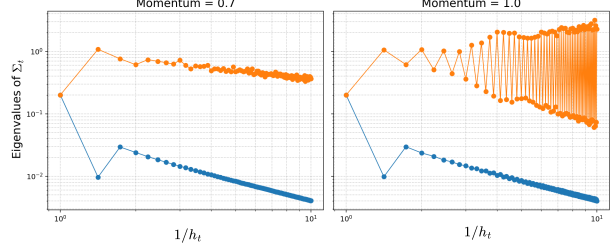


Figure 4. Comparison of the eigenvalue decay of Σ_t for Local EGOP Learning with and without momentum. On the left, we set $\beta = 0.7$, on the right $\beta = 1$ (no momentum). Without momentum, the second order eigenvalues are prone to wild oscillations.

terms, as well as the estimation error, make the $\sqrt{h_t}$ rate become unstable. We demonstrate the resulting localizations with and without momentum in Figure 4.

This leads to the following result.

Theorem 2 (Second Order Anisotropy). *Let H be invertible and Σ_t satisfy the recurrence in equation 2, $\sqrt{h_t} = \alpha r^t$, $0 < r < 1$, $\beta > 0$. Then, for α sufficiently small, $g^T\Sigma_t g = \Theta(h_t)$, and for $v \perp g$, $v^T\Sigma_t v = \Theta(\sqrt{h_t})$. It follows that, selecting $t_n = \frac{4 \log n}{(D+5) \log(1/r)}$,*

$$\mathbb{E} \left[\int (\hat{P}_{M_{t_n}}(f) - f)^2 d\mu_{t_n} \right] = O \left(n^{-\frac{4}{D+5}} \right).$$

Compared to a vanilla 0-order local polynomial estimator, this method nearly squares the asymptotic error, effectively cutting the effective dimension in half for D large. In our theory, we assume the initial localization has small covariance αI . In the resulting application of Lemma 3, this results in an explicit recurrence up to a higher-order remainder. While a useful theoretical construct, this is not necessary empirically, and we leave it to future research for a complete analysis of the iteration stability.

4.4.3. NOISY MANIFOLD

In the noisy manifold setting, we strengthen Lemma 3.

Lemma 4 (Noisy Manifold Taylor Expansion). *Let $g = \nabla f(x^*)$, $H = \nabla^2 f(x^*)$, $p = \pi(x^*)$, $\mathcal{T} := \mathcal{T}_p$, $\mathcal{N} := \mathcal{N}_p$, and T, R be as in Lemma 3. There exist non-negative constants C_N and $C_{\mathcal{T}N}$ such that, for all $A \succeq 0$,*

$$\|\pi_N R(A)\pi_N\| \leq C_N \|\pi_{\mathcal{T}} A \pi_{\mathcal{T}}\|^2, \quad (7)$$

$$\|\pi_{\mathcal{T}} R(A)\pi_N\| \leq C_{\mathcal{T}N} \|\pi_{\mathcal{T}} A \pi_{\mathcal{T}}\|. \quad (8)$$

Additionally, $\text{rank}(H) \leq 2d$.

We will leverage this weak orthogonal dependence to show that μ_t elongates along the space \mathcal{N}_{x^*} orthogonal to the manifold. However, while the function is constant on this fiber, its gradient is not. Indeed, we are only guaranteed that

the gradient remains tangent. Due to the effects of curvature, $\nabla f(p + v)$ may shrink or grow along different coordinate directions. We characterize this precisely as follows.

Lemma 5 (Gradient Geometry). *Let $p \in \mathcal{M}$, $\eta \in \mathcal{N}_p$, and $\|\eta\| < \tau$, where τ denotes the reach of \mathcal{M} . For S_p the shape operator,*

$$\nabla f(p + \eta) = (I - S_p(\eta))^{-1} \nabla f(p).$$

For any such η , there exists a subspace $\text{Null} = \text{Null}_{p+\eta}$ of dimension at least $D - 2d$ such that, for any $v, z \in \text{Null}$, $\nabla f(p + \eta + v) = \nabla f(p + \eta)$, $\nabla^2 f(p + \eta + v)z = 0$.

These geometric implications allow us to further adapt Lemma 4 to our geometry.

Corollary 1 (Shifted Taylor). *Let $x^* = p + \eta$, $v \in \text{Null}_{p+\eta}$. Define μ_v as the measure $\mu = N(x^*, \Sigma)$ conditioned on $\pi_{\text{Null}}[X - x^*] = v$, i.e. the draws where the Null component is fixed at v . Let Σ_v be the covariance of this distribution. Then,*

$$\mathcal{L}(\mu_v) = gg^T + H_v \Sigma_v H_v + g T_v(\Sigma_v)^T + T_v(\Sigma_v)g^T + R_v(\Sigma_v)$$

where $\text{Null} \subseteq \text{nullspace}(H_v)$, $\sup_{v \in \text{Null}} \|R_v(A)\| \leq C_{\text{Null}} \|A\|^2$, $T_v(A) \leq C_{\text{Null}} \|A\|$ for a uniform constant C_{Null} , and H_v, T_v, R_v are continuous in v and Lipschitz in $\|A\|$.

This allows us to perform an iterated integration, freezing the Taylor expansion along this shifted base point while preserving the fundamental first order behavior. To simplify our argument we assume that the covariance cap ζ is small, allowing a simple reduction of the dynamics to the non-degenerate case. This greatly streamlines the analysis, although we do not believe it is fundamental to the convergence.

Theorem 3 (Intrinsic Learning Rate). *Assume that $D \geq 2d$ and $\text{rank}(H) = 2d$. Let Σ_t satisfy the recurrence in equation 2, $\sqrt{h_t} = \alpha r^t$, $0 < r < 1$, $\beta > 0$. Then, for α, ζ sufficiently small, $g^T \Sigma_t g = \Theta(h_t)$. If $v \in \text{Null}$, then $v^T \Sigma_t v = \Theta(1)$, and if $\eta \in \text{Null}^\perp \cap g^\perp$, $\eta^T \Sigma \eta = \Theta(\sqrt{h_t})$. It follows that, selecting $t_n = \frac{4 \log n}{(2d+5) \log(1/r)}$,*

$$\mathbb{E} \left[\int (\hat{P}_{M_{t_n}}(f) - f)^2 d\mu_{t_n} \right] = O \left(n^{-\frac{4}{2d+5}} \right).$$

Rather than fully denoising the manifold, our analysis reveals that the manifold tangent, as well as the normal vectors that do not fall in Null , are subject to the same second-order anisotropy as observed in the full rank setting. These compose precisely those directions in which the gradient varies at first order. The resulting rate is comparable to that of a standard estimator applied to a completely denoised manifold, yielding an effective dimension of $d + 1/2$.

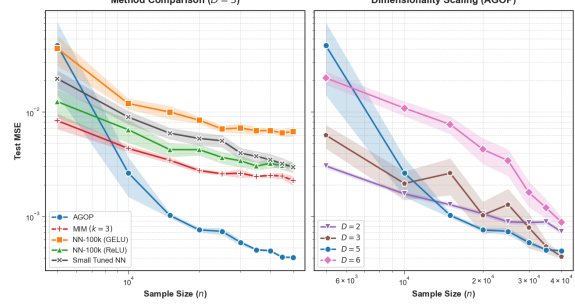


Figure 5. (Left) Comparison of Local EGOP Learning to the performance of two-layer neural network architectures trained on helical data in ambient dimension $D = 5$. (Right) Local EGOP Learning trained on helical data in various ambient dimensions D .

Example 3 (Multi-Index Learning). When the underlying manifold \mathcal{M} is flat, the supervised noisy manifold hypothesis reduces to a multi-index setting. The key distinction is that displacement away from the manifold not only preserves the function value, but also all higher order function derivatives. In particular, the Hessian has rank no more than d . When performing expansions such as Corollary 1, the orthogonal has no contribution to the EGOP, yielding a learning rate of $(d + 1)/2$.

Example 4 (Continuous Single-Index). When the underlying manifold is 1-dimensional, the tangent space coincides with the span of the gradient, hence $\pi_{g^\perp} H \pi_{g^\perp} = 0$, removing the second order anisotropy. Thus no normal directions contract asymptotically, leading to an effective dimension of 1 for the learning rate. This corroborates the result of Wu & Maggioni (2024).

5. Experiments

Details for data generation, evaluation, and training of each method can be found in Appendix A.

5.1. Two-layer Neural Network

We assess a variety of two-layer neural network architectures, with details in Appendix A. The covariate distribution is drawn from helical data, which is continuous single-index, being drawn from a noise contaminated curve, as well as multi-index 2 for D even, and 3 for D odd. Further, by construction it is well-approximated by a low intrinsic dimensional manifold, a typical setting for accelerated learning rates (Kiani et al. (2024); Liu et al. (2021), etc.).

As demonstrated in Figure 5, the two-layer neural networks readily adapt to the multi-index data structure. For $D = 5$, the overparameterized ReLU network achieves comparable error to a multi-index architecture pre-specified to learn a 3-dimensional subspace. However, Local EGOP Learning vastly reduces the error for moderate to large sample sizes.

This suggests that no architecture was able to fully adapt to the intrinsic continuous single-index structure.

5.2. Learning Rate

We generate helical data in a variety of dimensions, testing the Local EGOP Learning algorithm. As seen in Figure 5, the asymptotic learning rate has little dimensional dependence. However, error scaling depends strongly on whether D is even or odd, and this is because the underlying manifold changes in these settings, although its intrinsic dimension does not.

5.3. Feature Learning

In this section, we compare the local feature learning capabilities of a deep transformer-based neural network (Gorishniy et al., 2023) to Local EGOP Learning. We consider data generated from a 1-sphere under the supervised noisy manifold hypothesis. On this simple dataset, both algorithms result in nearly complete denoising of the data, as shown in Figures 3a and 3b. In Appendix A, we provide additional unsupervised embeddings for comparison.

5.4. Predicting the backbone angles in Molecular Dynamics (MD) data

Our final example comes from the analysis of molecular geometries. The raw data consist of X, Y, Z coordinates for each of the N_a atoms of a molecule, which, due to interatomic interactions, lie near a low-dimensional manifold (Das et al., 2006). While the governing equations of the simulated dynamics are unknown, for small organic molecules, certain backbone angles (Das et al., 2006) have been observed to vary along the aforementioned low-dimensional manifold. Specifically, for the malonaldehyde molecule, the two backbone angles denoted $\tau_{1,2}$ are shown in Figure 6b. We used a subsample of molecular configurations of size $n = 10^4$ from the MD simulation data of Chmiela et al. (2017) as input data. The configuration data, pre-processed as in Koelle et al. (2022), consist of $D = 50$ dimensional vectors and lie near a 2-dimensional surface with a torus topology (see Figure 6b). On a hold-out set of 500 test points, Local EGOP Learning yields an MSE of 0.00043, compared to 0.012 for Gaussian kernel Nadaraya-Watson with cross-validated bandwidth selection.

6. Discussion and Future Work

The problem of learning an EGOP (Trivedi et al., 2014; Radhakrishnan et al., 2025), its local counterpart (Takeda et al., 2007), or gradients (Mukherjee et al., 2010; Wu et al., 2010), has been a topic of frequent theoretical interest, with applications to image processing (Takeda et al., 2007; 2008), machine learning (Radhakrishnan et al., 2022; Beaglehole

et al., 2023), and dimension reduction (Yuan et al., 2023). Our research establishes a new functional framework to understand these methods, directly relating the EGOP to the MSE learning objective, and recursive kernel learning to a greedy variance reduction strategy. The resulting algorithm yields not only new efficiency guarantees for point estimation, but also tractable access to a local EGOP metrization.

In this paper, we introduce continuous index learning and the closely related supervised noisy manifold hypothesis. We demonstrate that Local EGOP Learning is able to achieve an intrinsic dimensional learning rate for such data. For generic manifolds, however, it does not completely denoise the covariate distribution. Our theory shows that a small subspace of the orthogonal will contract at the same rate as the tangent, despite the invariance of f . This counterintuitive result reflects the fact that our EGOP optimization scheme is derived via an upper-bound on the bias, and is thus not always sharp. The refinement of this methodology to close this gap is thus of both practical and theoretical importance.

The Local EGOP Learning algorithm is *adaptive*, in that it outperforms standard kernel regression algorithms when the noisy supervised manifold hypothesis fails to hold (Theorem 2), and yields an intrinsic dimensional rate when f is structured. In neither case is knowledge of the regularity of f or the latent manifold required to enhance estimation quality. Importantly, this means that users may use the algorithm without a priori knowledge of problem dimensionality, noise level, or whether the supervised manifold hypothesis holds.

Algorithm 1 was presented for clarity, not efficiency; there are many possible computational improvements, including partitioning schemes as in Beaglehole et al. (2025). Local EGOP Learning is based firmly on a MSE formulation of regression, restricting its utility to ℓ_2 loss. This method requires suitable modification to be applied directly to problems such as classification or image generation. This leaves open how an appropriate adaptation should be formulated in these settings.

Our methodology is primarily framed through a second order, Gaussian relaxation. One promising direction is to drop this restriction, and view $W(\mu_t)$ and $\Sigma(\mu_t)$ as functionals, and to then optimize the MSE using a Wasserstein gradient flow (Ambrosio et al., 2006) or other methods that operate at the distribution level. In particular, this would allow for non-ellipsoidal localizations, potentially allowing for improved learning rates in settings where the level-set is curved. A fundamental hurdle for any of these approaches is that, generally, the EGOP form can only upper bound localization-induced bias, and the resulting bound is not always sharp.

ACKNOWLEDGEMENTS

The authors would like to thank Misha Belkin for the initial suggestion of comparing Local EGOP Learning to the performance of two-layer neural networks, and Brennan Dury for suggestions and experiments related to earlier conceptions of this research.

References

Aamari, E. and Levraud, C. Non-asymptotic rates for manifold, tangent space, and curvature estimation, 2018. URL <https://arxiv.org/abs/1705.00989>.

Abbe, E., Boix-Adsera, E., and Misiakiewicz, T. The merged-staircase property: a necessary and nearly sufficient condition for sgd learning of sparse functions on two-layer neural networks, 2024. URL <https://arxiv.org/abs/2202.08658>.

Ambrosio, L., Gigli, N., and Savare, G. *Gradient Flows: In Metric Spaces and in the Space of Probability Measures*. Lectures in Mathematics. ETH Zürich. Birkhäuser Basel, 2006. ISBN 9783764373092. URL https://books.google.com/books?id=Hk_wNp0sc4gC.

Arnaboldi, L., Dandi, Y., Krzakala, F., Pesce, L., and Stephan, L. Repetita iuvant: Data repetition allows sgd to learn high-dimensional multi-index functions. *arXiv preprint arXiv:2405.15459*, 2024.

Aswani, A., Bickel, P., and Tomlin, C. Regression on manifolds: Estimation of the exterior derivative. *The Annals of Statistics*, 39(1):48–81, February 2011. doi: 10.1214/10-AOS834.

Bakry, D., Gentil, I., and Ledoux, M. *Analysis and geometry of Markov diffusion operators*, volume 348. Springer Science & Business Media, 2013.

Barla, A., Odone, F., and Verri, A. Hausdorff kernel for 3d object acquisition and detection. In *Computer Vision—ECCV 2002: 7th European Conference on Computer Vision Copenhagen, Denmark, May 28–31, 2002 Proceedings, Part IV* 7, pp. 20–33. Springer, 2002.

Beaglehole, D., Radhakrishnan, A., Pandit, P., and Belkin, M. Mechanism of feature learning in convolutional neural networks. *arXiv preprint arXiv:2309.00570*, 2023.

Beaglehole, D., Holzmüller, D., Radhakrishnan, A., and Belkin, M. xrfm: Accurate, scalable, and interpretable feature learning models for tabular data. *arXiv preprint arXiv:2508.10053*, 2025.

Belkin, M., Ma, S., and Mandal, S. To understand deep learning we need to understand kernel learning. In *International Conference on Machine Learning*, pp. 541–549. PMLR, 2018.

Bietti, A., Bruna, J., Sanford, C., and Song, M. J. Learning single-index models with shallow neural networks. *Advances in neural information processing systems*, 35: 9768–9783, 2022.

Bigoni, D., Marzouk, Y., Prieur, C., and Zahm, O. Nonlinear dimension reduction for surrogate modeling using gradient information. *Information and Inference: A Journal of the IMA*, 11(4):1597–1639, 2022.

Boix-Adsera, E., Littwin, E., Abbe, E., Bengio, S., and Susskind, J. Transformers learn through gradual rank increase. *Advances in Neural Information Processing Systems*, 36:24519–24551, 2023.

Breiman, L. and Meisel, W. S. General estimates of the intrinsic variability of data in nonlinear regression models. *Journal of the American Statistical Association*, 71(354): 301–307, 1976.

Bush, J. C4l image dataset, 2021. URL <https://dx.doi.org/10.21227/bc9m-f507>.

Chadebec, C. and Allassonnière, S. A geometric perspective on variational autoencoders, 2022. URL <https://arxiv.org/abs/2209.07370>.

Chapelle, O., Haffner, P., and Vapnik, V. N. Support vector machines for histogram-based image classification. *IEEE transactions on Neural Networks*, 10(5):1055–1064, 1999.

Chmiela, S., Tkatchenko, A., Sauceda, H., Poltavsky, I., Schütt, K. T., and Müller, K.-R. Machine learning of accurate energy-conserving molecular force fields. *Science Advances*, March 2017.

Coifman, R. R. and Lafon, S. Diffusion maps. *Applied and computational harmonic analysis*, 21(1):5–30, 2006.

Cui, T., Tong, X., and Zahm, O. Optimal riemannian metric for poincaré inequalities and how to ideally precondition langevin dynamics. *arXiv preprint arXiv:2404.02554*, 2024.

Damian, A., Nichani, E., Ge, R., and Lee, J. D. Smoothing the landscape boosts the signal for sgd: Optimal sample complexity for learning single index models. *Advances in Neural Information Processing Systems*, 36:752–784, 2023.

Das, P., Moll, M., Stamat, H., Kavraki, L., and Clementi, C. Low-dimensional, free-energy landscapes of protein-folding reactions by nonlinear dimensionality reduction. *Proceedings of the National Academy of Sciences*, 103 (26):9885–9890, 2006.

Do Carmo, M. P. *Differential geometry of curves and surfaces: revised and updated second edition*. Courier Dover Publications, 2016.

El Karoui, N. The spectrum of kernel random matrices. *The Annals of Statistics*, 38(1):1–50, feb 2010. doi: 10.1214/09-AOS720.

Federer, H. Curvature measures. *Transactions of the American Mathematical Society*, 93(3):418–491, 1959.

Friedman, J. H. A tree-structured approach to nonparametric multiple regression. In *Smoothing Techniques for Curve Estimation: Proceedings of a Workshop held in Heidelberg, April 2–4, 1979*, pp. 5–22. Springer, 1979.

Garcia Trillos, N. Variational limits of k-nn graph-based functionals on data clouds. *SIAM Journal on Mathematics of Data Science*, 1(1):93–120, 2019.

Genovese, C. R., Perone-Pacifico, M., Verdinelli, I., and Wasserman, L. A. Minimax manifold estimation. *Journal of Machine Learning Research*, 13: 1263–1291, 2012. URL <http://dl.acm.org/citation.cfm?id=2343687>.

Genton, M. G. Classes of kernels for machine learning: a statistics perspective. *Journal of machine learning research*, 2(Dec):299–312, 2001.

Gong, A., Choi, K., and Dwivedi, R. Supervised kernel thinning. *arXiv preprint arXiv:2410.13749*, 2024.

Gorishniy, Y., Rubachev, I., Khrulkov, V., and Babenko, A. Revisiting deep learning models for tabular data. *Advances in neural information processing systems*, 34: 18932–18943, 2021.

Gorishniy, Y., Rubachev, I., and Babenko, A. On embeddings for numerical features in tabular deep learning, 2023. URL <https://arxiv.org/abs/2203.05556>.

Heise, D. R. Multivariate model building: The validation of a search strategy., 1971.

Hristache, M., Juditsky, A., Polzehl, J., and Spokoiny, V. Structure adaptive approach for dimension reduction. *Annals of Statistics*, pp. 1537–1566, 2001.

Isserlis, L. On a formula for the product-moment coefficient of any order of a normal frequency distribution in any number of variables. *Biometrika*, 12(1/2):134–139, 1918.

Jacot, A., Gabriel, F., and Hongler, C. Neural tangent kernel: Convergence and generalization in neural networks. *Advances in neural information processing systems*, 31, 2018.

Joachims, T. Text categorization with support vector machines: Learning with many relevant features. In *European conference on machine learning*, pp. 137–142. Springer, 1998.

Juditsky, A. B., Lepski, O. V., and Tsybakov, A. B. Nonparametric estimation of composite functions. *The Annals of Statistics*, 37(3):1360–1404, 2009. doi: 10.1214/08-AOS611.

Kiani, B., Wang, J., and Weber, M. Hardness of learning neural networks under the manifold hypothesis. *Advances in Neural Information Processing Systems*, 37:5661–5696, 2024.

Koelle, S., Zhang, H., Meilă, M., and Chen, Y.-C. Manifold coordinates with physical meaning. *Journal of Machine Learning Research*, 23, 2022.

Kokot, A. and Luedtke, A. Coreset selection for the sinkhorn divergence and generic smooth divergences. *arXiv preprint arXiv:2504.20194*, 2025.

Kokot, A., Murad, O.-V., and Meila, M. The noisy laplacian: a threshold phenomenon for non-linear dimension reduction. In *Forty-second International Conference on Machine Learning*, 2025.

Kondor, R. and Jebara, T. A kernel between sets of vectors. In *Proceedings of the 20th international conference on machine learning (ICML-03)*, pp. 361–368, 2003.

Landa, B. and Cheng, X. Robust inference of manifold density and geometry by doubly stochastic scaling. *SIAM Journal on Mathematics of Data Science*, 5(3):589–614, 2023.

Lee, J. D., Oko, K., Suzuki, T., and Wu, D. Neural network learns low-dimensional polynomials with sgd near the information-theoretic limit. *Advances in Neural Information Processing Systems*, 37:58716–58756, 2024.

Lee, K.-Y., Li, B., and Chiaromonte, F. A general theory for nonlinear sufficient dimension reduction: Formulation and estimation. *The Annals of Statistics*, pp. 221–249, 2013.

Liu, H., Chen, M., Zhao, T., and Liao, W. Besov function approximation and binary classification on low-dimensional manifolds using convolutional residual networks. In *International Conference on Machine Learning*, pp. 6770–6780. PMLR, 2021.

Lowe, D. G. Object recognition from local scale-invariant features. In *Proceedings of the seventh IEEE international conference on computer vision*, volume 2, pp. 1150–1157. Ieee, 1999.

Mei, W. and Bullo, F. Lasalle invariance principle for discrete-time dynamical systems: A concise and self-contained tutorial. *arXiv preprint arXiv:1710.03710*, 2017.

Mischaikow, K., Smith, H., and Thieme, H. R. Asymptotically autonomous semiflows: chain recurrence and lyapunov functions. *Transactions of the American Mathematical Society*, 347(5):1669–1685, 1995.

Mousavi-Hosseini, A., Park, S., Girotti, M., Mitliagkas, I., and Erdogdu, M. A. Neural networks efficiently learn low-dimensional representations with sgd. *arXiv preprint arXiv:2209.14863*, 2022.

Mukherjee, S., Wu, Q., and Zhou, D.-X. Learning gradients on manifolds. 2010.

Nouy, A. and Pasco, A. Surrogate to poincaré inequalities on manifolds for dimension reduction in nonlinear feature spaces. *arXiv preprint arXiv:2505.01807*, 2025.

Odene, F., Barla, A., and Verri, A. Building kernels from binary strings for image matching. *IEEE Transactions on Image Processing*, 14(2):169–180, 2005.

Osborne, M. *Bayesian Gaussian processes for sequential prediction, optimisation and quadrature*. PhD thesis, Oxford University, UK, 2010.

Radhakrishnan, A., Beaglehole, D., Pandit, P., and Belkin, M. Mechanism of feature learning in deep fully connected networks and kernel machines that recursively learn features. *arXiv preprint arXiv:2212.13881*, 2022.

Radhakrishnan, A., Belkin, M., and Drusvyatskiy, D. Linear recursive feature machines provably recover low-rank matrices. *Proceedings of the National Academy of Sciences*, 122(13):e2411325122, 2025.

Rao, B. P. *Nonparametric functional estimation*. Academic press, 2014.

Samarov, A. M. Exploring regression structure using non-parametric functional estimation. *Journal of the American Statistical Association*, 88(423):836–847, 1993.

Schmid, C. and Mohr, R. Local grayvalue invariants for image retrieval. *IEEE transactions on pattern analysis and machine intelligence*, 19(5):530–535, 1997.

Schölkopf, B., Simard, P., Smola, A., and Vapnik, V. Prior knowledge in support vector kernels. *Advances in neural information processing systems*, 10, 1997.

Scornet, E. Random forests and kernel methods. *IEEE Transactions on Information Theory*, 62(3):1485–1500, 2016.

Shen, G., Jiao, Y., Lin, Y., Horowitz, J. L., and Huang, J. Deep quantile regression: Mitigating the curse of dimensionality through composition. *arXiv preprint arXiv:2107.04907*, 2021.

Stein, C. M. Estimation of the mean of a multivariate normal distribution. *The annals of Statistics*, pp. 1135–1151, 1981.

Takeda, H., Farsiu, S., and Milanfar, P. Kernel regression for image processing and reconstruction. *IEEE Transactions on image processing*, 16(2):349–366, 2007.

Takeda, H., Farsiu, S., and Milanfar, P. Deblurring using regularized locally adaptive kernel regression. *IEEE transactions on image processing*, 17(4):550–563, 2008.

Thompson, A. C. On certain contraction mappings in a partially ordered vector space. *Proceedings of the American Mathematical Society*, 14(3):438–443, 1963.

Trivedi, S., Wang, J., Kpotufe, S., and Shakhnarovich, G. A consistent estimator of the expected gradient outerproduct. In *UAI*, pp. 819–828, 2014.

Tsybakov, A. B. *Nonparametric estimators*, pp. 1–76. Springer New York, New York, NY, 2009. ISBN 978-0-387-79052-7. doi: 10.1007/978-0-387-79052-7_1. URL https://doi.org/10.1007/978-0-387-79052-7_1.

Verdière, R., Prieur, C., and Zahm, O. Diffeomorphism-based feature learning using poincaré inequalities on augmented input space. *Journal of Machine Learning Research*, 26(139):1–31, 2025.

Vishwanathan, S. V. N., Schraudolph, N. N., Kondor, R., and Borgwardt, K. M. Graph kernels. *The Journal of Machine Learning Research*, 11:1201–1242, 2010.

Wainwright, M. J. *High-dimensional statistics: A non-asymptotic viewpoint*, volume 48. Cambridge university press, 2019.

Wallraven, Caputo, and Graf. Recognition with local features: the kernel recipe. In *Proceedings Ninth IEEE International Conference on Computer Vision*, pp. 257–264. IEEE, 2003.

Wu, Q., Guinney, J., Maggioni, M., and Mukherjee, S. Learning gradients: predictive models that infer geometry and statistical dependence. *The Journal of Machine Learning Research*, 11:2175–2198, 2010.

Wu, Y. and Maggioni, M. Conditional regression for the nonlinear single-variable model. *arXiv preprint arXiv:2411.09686*, 2024.

Xia, Y., Tong, H., Li, W. K., and Zhu, L.-X. An adaptive estimation of dimension reduction space. *Journal of the Royal Statistical Society Series B: Statistical Methodology*, 64(3):363–410, 2002.

Yeh, Y.-R., Huang, S.-Y., and Lee, Y.-J. Nonlinear dimension reduction with kernel sliced inverse regression. *IEEE transactions on Knowledge and Data Engineering*, 21(11):1590–1603, 2008.

Yuan, G., Xu, M., Kpotufe, S., and Hsu, D. Efficient estimation of the central mean subspace via smoothed gradient outer products. *arXiv preprint arXiv:2312.15469*, 2023.

Zhu, L., Davis, D., Drusvyatskiy, D., and Fazel, M. Iteratively reweighted kernel machines efficiently learn sparse functions. *arXiv preprint arXiv:2505.08277*, 2025.

Local EGOP for Continuous Index Learning: Supplementary Material

A. Experiment Details

The simulations were run on a machine of Intel® Xeon® processors with 48 CPU cores, and 50GB of RAM.

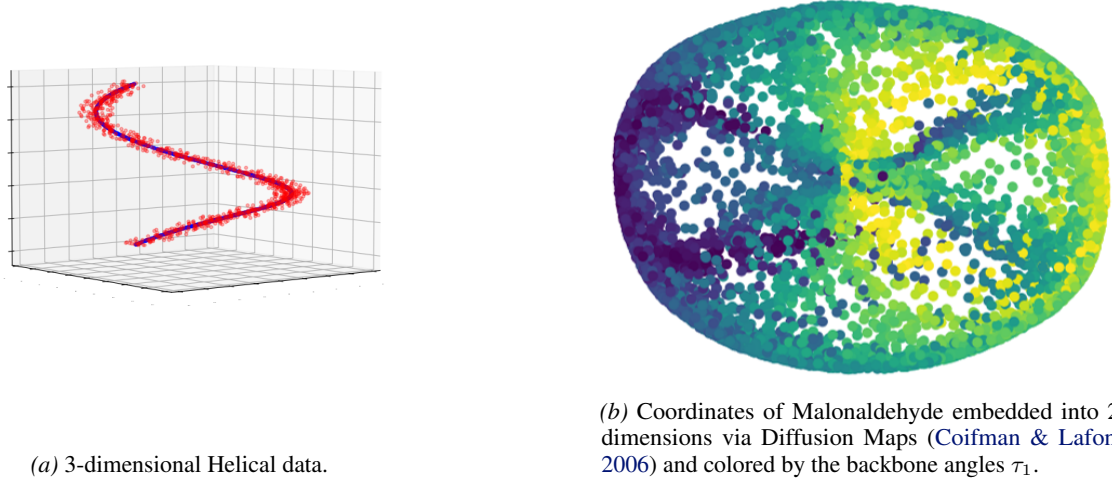


Figure 6. Visualizations of the experimental datasets.

A.1. General Set-up

The following simulations to empirically justify our theoretical results. First, expanding on the noisy manifold setting, we show how the regression error rates of Local EGOP Learning remain invariant to the injection of high-dimensional noise. We demonstrate that two-layer neural networks are not able to efficiently learn in the noisy manifold setting, with a sharp decrease in performance compared to Local EGOP Learning. We next compare the performance of our method to that of a deep neural network on toy data. In particular, we show how the feature embeddings produced by transformers trained on a simple example are qualitatively similar to the localizations generated by our procedure. Finally, we apply this procedure to estimate backbone angles in Molecular Dynamics (MD) data, where we leverage the noisy manifold structured data to improve prediction quality.

In our simulations, we consider helical data, parameterized by a curve $\theta(t) = (\sin(t + w_1), \cos(t + w_1), \sin(t + w_2), \cos(t + w_2), \dots, g(t))$, where $g(t) = t$ is a linear term included if D is odd dimensional, and the w_i are constant offsets taken as a mesh from 0 to 2π . We rescale this data by a constant τ , then contaminate it with uniform orthogonal noise of radius r . In our simulations, we set $\tau = 0.8$, $r = 0.5$, and sample t from 0 to 2π . See Figure 6a for a visualization. For the outcomes y , we generate a third-degree polynomial with coefficients uniformly sampled from $(-3, 3)$, then evaluate it at the projection point onto $\theta(t)$.

In our synthetic experiments, to generate labeled data we randomly generated a homogeneous cubic polynomial

$$f(x) = \sum_{|\alpha| \leq 3} c_\alpha x^\alpha,$$

where $c_\alpha \sim \text{Uniform}[-3, 3]$. The resulting function f is then evaluated at the unperturbed datapoints before the features X were contaminated with noise orthogonal to the underlying manifold \mathcal{M} . The coefficients c_α are randomly sampled across each replicate of the experiments. In our plots, confidence bands are displayed with a width of ± 1 standard error. We generically apply the below hyperparameters to the Local EGOP Learning algorithm in each example.

- Number of EGOP iterations $T_{\text{test}} = 150$,
- Monte Carlo sample size $m = 300$,
- Bandwidth decay $h_t = (1 + t)^{-1.2}$,
- Initialization scale $\alpha = 0.2$,
- Exclusion radius $\varepsilon = 1.6$.

A.2. Two-layer Neural Network

We train fully connected NNs with both ReLU and GELU activations. All first layers use Kaiming initialization, and output layers are initialized at variance $1/\sqrt{m}$ where m is hidden width. All networks are trained with Adam.

For moderate-scale neural models, we conduct a grid search over hyperparameters. Widths are selected from $\{128, 256, 512, 1024, 2048, 4096, 8192\}$, learning rates are selected from $\{10^{-3}, 3 \times 10^{-3}\}$, weight decay from $\{0, 10^{-5}, 10^{-4}\}$, and batch size from $\{16, 32, 64\}$. The default Adam momentum parameters are used. Early stopping is applied with patience 200 and improvement tolerance 10^{-4} monitored on a validation split. In each experiment, only the optimal test error of these methods is aggregated into the ‘‘Small Tuned NN’’ plot.

We train overparameterized two-layer models with width 100,000, Adam with learning rate 0.003, batch size 64, and fixed weight decay 10^{-4} , applying early stopping with patience 300 and improvement tolerance 10^{-4} .

We also consider multi-index models $f(x) = g(Ux)$, g a two-layer NN, with width 256 and GELU activations, U a rank three projection matrix updated at each iteration.

A.3. Feature Learning

We generated $n = 50,000$ samples on a spherical cap in \mathbb{R}^2 , restricted to an angular width of 25° . Each point x_i , we evaluate $f(x_i)$ for f a cubic polynomial with Uniform $[-1, 1]$ coefficients. The features x_i are then scaled radially by a random factor $r_i \sim \text{Uniform}[r, R]$, with $r = 0.6$ and $R = 1.8$. Additive Gaussian noise with standard deviation 0.05 was applied to the labels. We set $x^* = (1, 0)^T$.

We trained an FTTransformer regression model (Gorishniy et al., 2021) on this dataset using the `rtdl` and `zero` frameworks. The network was trained for 40 epochs with a batch size of 1024 and learning rate 2×10^{-3} . After every 50 training steps, we computed weights:

$$w_i = \frac{\exp(-\|z_i - z^*\|^2/8)}{\sum_j \exp(-\|z_j - z^*\|^2/8)},$$

where z_i denotes the learned feature representation of x_i .

A.4. Unsupervised Embedding

As noted in works such as (Coifman & Lafon, 2006; El Karoui, 2010; Landa & Cheng, 2023; Kokot et al., 2025), unsupervised methods such as diffusion maps are robust to noise. The resulting low-frequency eigenfunctions closely match those of the underlying manifold. However, as demonstrated in Figure 7, they fail to capture this structure exactly, and thus cannot match the metrization produced by Local EGOP Learning and deep learning architectures in Figure 3a.

B. Proofs

In our theory, we focus on the kernel $k = \exp(-\|x\|^2)$. We discuss general kernels in Appendix B.1.4.

B.1. Bias Control via EGOP

B.1.1. BIAS BOUND

To derive the upper bound from Lemma 1, we argue in stages. We first decompose the kernel smoother into two parts. The first is given by a pure Gaussian convolution and a density dependent covariance relating f and p . Both terms can readily

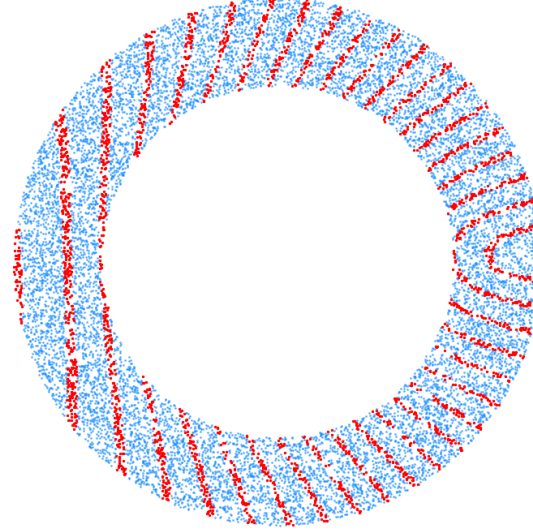


Figure 7. Data sampled from an annulus, with red rings displaying uniform distances in diffusion map embedding distance from the point $(1, 0)^T$, for a 2-dimensional embedding.

be controlled via the EGOP form, leading to our bound. In the following, we absorb the bandwidth into the metric and covariance, suppressing h in the notation.

Define $\mu_M := N(x^*, M^{-1})$, $\mathbb{E}_M[\cdot] := \mathbb{E}_{\mu_M}[\cdot]$, Cov_M , Var_M similarly.

Lemma 6 (Basic Decomposition).

$$P_M f = \mathbb{E}_M f + \frac{\text{Cov}_M[f, p]}{\mathbb{E}_M p} =: G_M f + A_M f$$

Proof. We can simply compute

$$\begin{aligned} P_M f &= \frac{\mathbb{E}_M[f p]}{\mathbb{E}_M[p]} = \frac{\mathbb{E}_M[f] \mathbb{E}_M[p]}{\mathbb{E}_M[p]} + \frac{\text{Cov}_M[f, p]}{\mathbb{E}_M[p]} \\ &= \mathbb{E}_M[f] + \frac{\text{Cov}_M[f, p]}{\mathbb{E}_M[p]} =: G_M f + A_M f. \end{aligned}$$

□

Lemma 7 (Gaussian Poincaré).

$$\int (\mathbb{E}_M[f] - f)^2 d\mu_M \leq W(\mu_M)$$

Proof. This is simply the Gaussian Poincaré inequality, see for instance (Bakry et al., 2013)[Proposition 4.1.1]. □

Lemma 8 (Poincaré \times p variance).

$$(A_M f)^2 \leq W(\mu_M) \frac{\text{Var}_M(p)}{\mathbb{E}_M[p]^2}$$

Proof.

$$A_M f^2 = \frac{\text{Cov}_M[f, p]^2}{\mathbb{E}_M[p]^2} \leq \frac{\text{Var}_M(f) \text{Var}_M(p)}{\mathbb{E}_M[p]^2} \leq W(\mu_M) \frac{\text{Var}_M(p)}{\mathbb{E}_M[p]^2},$$

applying the Gaussian Poincaré inequality (Bakry et al., 2013)[Proposition 4.1.1] for the last line. □

Proof of Lemma 1. We can apply Lemmas 7 and 8 immediately to yield

$$\begin{aligned} \int (P_M - f)^2 d\mu_M &= \int (\mathbb{E}_M[f] - f + A_M f)^2 d\mu_M = \int (\mathbb{E}_M[f] - f)^2 d\mu_M + A_M f^2 \\ &\leq \left(1 + \frac{\text{Var}_M(p)}{\mathbb{E}_M[p]^2}\right) W(\mu_M). \end{aligned}$$

Note that the density dependent factor $\frac{\text{Var}_M(p)}{\mathbb{E}_M[p]^2}$ is bounded by the continuity of p and the capped covariance assumptions. \square

B.1.2. VARIANCE BOUND

We operate by a typical Nadaraya-Watson style argument. Our first steps are to show that the denominator of our estimator concentrates, allowing us to treat it as a constant up to a negligible residual. Let $\gamma_M \propto \det(M)^{1/2}$ by the normalization factor of μ_M . Define

$$\hat{C}'_M := \gamma_M \hat{C}_M := \gamma_M \frac{1}{n} \sum_{i=1}^n \exp(-\mathbf{(X}_i - \mathbf{x}^*)^T M(\mathbf{X}_i - \mathbf{x}^*)).$$

Lemma 9 (Denominator Concentration).

$$\mathbb{P}(|\hat{C}'_M - \mathbb{E}_M(p)| \leq \mathbb{E}_M(p)/2) \leq 2 \exp\left(-\frac{n\mathbb{E}_M(p)}{10\gamma_M}\right)$$

Proof. We prove this by applying Bernstein's inequality. First, observe $\mathbb{E}[\hat{C}_M] = G_M(p)$. Next, $\exp(-v^T M v) \in (0, 1]$ for any v , hence $\hat{C}'_M = \frac{\gamma_M}{n} \sum_{i=1}^n \exp(-\mathbf{(X}_i - \mathbf{x})^T M(\mathbf{X}_i - \mathbf{x}))$ is the sample mean of iid bounded random variables in $(0, \gamma_M]$. Further, we can compute

$$\begin{aligned} \text{Var}[\gamma_M \exp(-\mathbf{(X}_i - \mathbf{x})^T M(\mathbf{X}_i - \mathbf{x}))] &\leq \gamma_M \mathbb{E}[\gamma_M \exp(-\mathbf{(X}_i - \mathbf{x})^T M(\mathbf{X}_i - \mathbf{x}))^2] \\ &\leq \gamma_M \mathbb{E}[\exp(-\mathbf{(X}_i - \mathbf{x})^T M(\mathbf{X}_i - \mathbf{x}))] = \gamma_M G_M(p). \end{aligned}$$

Hence,

$$\begin{aligned} \mathbb{P}(|\hat{C}'_M - G_M(p)| \leq -G_M(p)/2) &\leq 2 \exp\left(-\frac{nG_M(p)^2}{8 \text{Var}(\gamma_M \exp(-\mathbf{(X}_i - \mathbf{x})^T M(\mathbf{X}_i - \mathbf{x}))) + \frac{4}{3}\gamma_M G_M(p)^2}\right) \\ &\leq 2 \exp\left(-\frac{nG_M(p)^2}{8\gamma_M G_M(p) + \frac{4}{3}\gamma_M G_M(p)}\right) \\ &\leq 2 \exp\left(-\frac{nG_M(p)}{10\gamma_M}\right). \end{aligned}$$

\square

Lemma 10 (Full Variance Expression). *Assume that the noise ε_i have finite fourth moments. Then, there exists a constant $C > 0$ such that*

$$\begin{aligned} \mathbb{E}[(\hat{P}_M(f) - P_M(f))^2] &\leq 2 \frac{\mathbb{E}[\gamma_M^2 \exp(-\mathbf{(X}_i - \mathbf{x})^T M(\mathbf{X}_i - \mathbf{x}))^2 \{Y_i - P_M(f)\}^2]}{nG_M(p)^2} \\ &\quad + 2 \frac{\mathbb{E}[\{\gamma_M \exp(-\mathbf{(X}_i - \mathbf{x})^T M(\mathbf{X}_i - \mathbf{x})) Y_i\}^2]}{nG_M(p)^2} + C \exp\left(-\frac{nG_M(p)}{10\gamma_M}\right) \end{aligned}$$

Proof. Let E be the event $|\hat{C}_M - G_M(p)| \leq G_M(p)/2$. We compute

$$\begin{aligned}\hat{P}_M(f) - P_M(f) &= \frac{\frac{1}{n} \sum_{i=1}^n \gamma_M \exp(-(X_i - x^*)^T M(X_i - x)) Y_i}{\hat{C}'_M} - \frac{G_M(f)p}{G_M(p)} \\ &= \frac{\frac{1}{n} \sum_{i=1}^n [\gamma_M \exp(-(X_i - x^*)^T M(X_i - x^*)) \{Y_i - P_M(f)\}]}{G_M(p)} \mathbf{1}_E \\ &\quad + \frac{G_M(p) - \hat{C}'_M}{G_M(p)\hat{C}'_M} \frac{1}{n} \sum_{i=1}^n [\gamma_M \exp(-(X_i - x^*)^T M(X_i - x^*)) Y_i] \mathbf{1}_E \\ &\quad + \left\{ \frac{\frac{1}{n} \sum_{i=1}^n \gamma_M \exp(-(X_i - x^*)^T M(X_i - x^*)) Y_i}{\hat{C}'_M} - \frac{G_M(f)p}{G_M(p)} \right\} \mathbf{1}_{E^c}.\end{aligned}$$

Hence,

$$\begin{aligned}\mathbb{E}[(\hat{P}_M(f) - P_M(f))^2] &\leq 2 \frac{\mathbb{E}[\gamma_M^2 \exp(-(X_i - x^*)^T M(X_i - x^*))^2 \{Y_i - P_M(f)\}^2]}{nP_M(p)^2} \\ &\quad + 2\mathbb{E} \left[\left\{ \frac{G_M(p) - \hat{C}'_M}{G_M(p)\hat{C}'_M} \frac{1}{n} \sum_{i=1}^n [\gamma_M \exp(-(X_i - x^*)^T M(X_i - x^*)) Y_i] \right\}^2 \mathbf{1}_E \right] \\ &\quad + 2\mathbb{E} \left[\left\{ \hat{P}_M(f) - P_M(f) \right\}^2 \mathbf{1}_{E^c} \right].\end{aligned}$$

The first term is as desired. Next, by definition of the event, we have

$$\mathbb{E} \left[\left\{ \frac{G_M(p) - \hat{C}'_M}{G_M(p)\hat{C}'_M} \frac{1}{n} \sum_{i=1}^n [\gamma_M \exp(-(X_i - x^*)^T M(X_i - x^*)) Y_i] \right\}^2 \mathbf{1}_E \right] \leq \frac{\mathbb{E}[\{\gamma_M \exp(-(X_i - x^*)^T M(X_i - x^*)) Y_i\}^2]}{nG_M(p)^2}.$$

For the remaining term, observe that

$$\hat{P}_M(f) = \sum_{i=1}^n w_i Y_i$$

where w_i are a convex combination. Hence,

$$\mathbb{E} \left[\left\{ \hat{P}_M(f) - P_M(f) \right\}^2 \mathbf{1}_{E^c} \right] \leq \sqrt{\mathbb{E} \left[\left\{ 2\hat{P}_M(f)^2 + 2P_M(f)^2 \right\}^2 \right]} \mathbb{P}[E^c] \leq C \exp \left(-\frac{nG_M(p)}{10\gamma_M} \right),$$

by Lemma 9 and the hypothesis on the moments of ε_i and the boundedness of f . \square

With this out of the way, we bound the two remaining expectations.

Lemma 11 (Normalization Constant). *There exists a constant $C > 0$ such that*

$$\begin{aligned}\mathbb{E}[\gamma_M^2 \exp(-(X_i - x^*)^T M(X_i - x^*))^2 \{Y_i - P_M(f)\}^2] &\leq C\gamma_M G_{2M}(p), \\ \mathbb{E}[\{\gamma_M \exp(-(X_i - x^*)^T M(X_i - x^*)) Y_i\}^2] &\leq C\gamma_M G_{2M}(p).\end{aligned}$$

Proof. Notice that $\gamma_M/\gamma_{4M} = C$ for some constant. Let $\varepsilon \sim \rho$. Focusing on the first expression,

$$\begin{aligned}\mathbb{E}[\gamma_M^2 \exp(-(X_i - x^*)^T M(X_i - x^*))^2 \{Y_i - P_M(f)\}^2] &= C\gamma_M \int \gamma_{4M} \exp(-(z - x)^T [2M](z - x)) p(y)(f(y) + \varepsilon - P_M(f))^2 dz d\rho(\varepsilon) \\ &= C\gamma_M \mathbb{E}_{2M}[p(x + Z) \mathbb{E}_\rho[(f(x + Z) + \mathcal{E} - P_M(f)(x))^2]] \leq C'\gamma_M G_{2M}(p)(x),\end{aligned}$$

using bounded moments and bounded f assumptions. Similarly,

$$\mathbb{E}[\{\gamma_M \exp(-(X_i - x^*)^T M(X_i - x^*)) Y_i\}^2] = C\gamma_M \mathbb{E}_{2M,\rho}[p(Z)[f(Z) + \mathcal{E}]^2] = C\gamma_M G_{2M}(p). \quad \square$$

Combining these yields the desired variance bound multiplied by density dependent factors.

Proof of Lemma 2. By Lemmas 10 and 11, there exists a constant $C > 0$ such that

$$\begin{aligned}\mathbb{E}[(\hat{P}_M(f) - P_M(f))^2] &\leq C \frac{\gamma_M}{n} \left(\frac{G_{2M}(p)}{G_M(p)^2} \right) + C \exp \left(-\frac{n}{\gamma_M} \left(\frac{G_M(p)}{10} \right) \right) \\ &= O \left(\frac{\sqrt{\det M}}{n} \right).\end{aligned}$$

□

B.1.3. MSE

We compile the results from the previous section to provide guarantees for the MISE against Gaussians.

Proof of Theorem 1. It follows immediately from Lemmas 1 and 2 that

$$\begin{aligned}\mathbb{E}_M[(\hat{P}_M(f) - f)^2] &\leq C \frac{\sqrt{\det M}}{n} \left(\frac{G_{2M}(p)}{G_M(p)^2} \right) + C \exp \left(-\frac{n}{\sqrt{\det M}} \left(\frac{G_M(p)}{10} \right) \right) + C \left(1 + \frac{\text{Var}_{M_t}(p(Z))}{G_{M_t}(p)^2} \right) W(\mu_M) \\ &= O \left(\frac{\sqrt{\det M_t}}{n} + W(\mu_t) \right).\end{aligned}$$

□

B.1.4. GENERAL KERNELS

In this section, we discuss which of results above are applicable to kernels of the form $k(M^{1/2}x)$. We start with the following Poincaré inequality. Let $\mu_{k,M}$ denote the probability distribution with density $\propto k(M^{1/2}[x - x^*])$.

Lemma 12 (Kernel Poincaré). *The measure $\mu_{k,M}$ has covariance proportionate to M^{-1} . If $\mu_{k,I}$ satisfies a Poincaré inequality with constant $1/C_I$, then*

$$\text{Var}_{\mu_{k,M}}(f) \leq \frac{1}{C_I} \int \nabla f^T M^{-1} \nabla f \, d\mu_{k,M}.$$

Proof. For convenience, we translate $x^* = 0$ without loss of generality. For the first claim, notice that when $M = I$, the density is symmetric about the origin, hence the covariance is proportionate to the identity. Thus the claim follows as $\mu_{k,M}$ is the pushforward of $\mu_{k,I}$ by $M^{-1/2}$.

Further,

$$\text{Var}_{\mu_{k,M}}(f) = \frac{1}{\sqrt{\det M}} \text{Var}_{\mu_{k,I}}(f \circ M^{-1/2}) \leq \frac{1}{C_I} \int \frac{1}{\sqrt{\det M}} \|\nabla f(M^{-1/2}y)\|^2 d\mu_{k,I}(y).$$

An application of the chain rule gives that

$$\nabla_y f(M^{-1/2}y) = M^{-1/2} \nabla f(M^{-1/2}y).$$

Hence,

$$\text{Var}_{\mu_{k,M}}(f) \leq \frac{1}{C_I} \int \frac{1}{\sqrt{\det M}} \|M^{-1/2} \nabla f(M^{-1/2}y)\|^2 \mu_{k,I}(y).$$

Changing variable back to $\mu_{k,M}$ yields the desired result. □

With this in hand, the following is immediate for \hat{P}_M with k generic. The claim for the covariance similarly follows by change of variables, after observing that $\mu_{k,I}$ is rotation invariant, and therefore has isotropic covariance.

Corollary 2 (Kernel MSE). *Take k to be nonnegative, and satisfying a Poincaré inequality for isotropic covariance. Assume that f is bounded and ε_i has finite fourth moments. Then there exists an absolute constant C such that*

$$\begin{aligned} \mathbb{E} \left[\int (\hat{P}_M(f) - f)^2 d\mu_{k,M} \right] \leq \\ C \frac{\sqrt{\det M}}{n} \left(\frac{\mathbb{E}_{\mu_{k,2M}}[p]}{\mathbb{E}_{\mu_{k,2M}}[p]^2} \right) + C \exp \left(-\frac{n}{\sqrt{\det M}} \left(\frac{\mathbb{E}_{\mu_{k,2M}}[p]}{10} \right) \right) + C \left(1 + \frac{\text{Var}_{\mu_{k,M}}(p)}{\mathbb{E}_{\mu_{k,M}}[p]^2} \right) W(\mu_{k,M}). \end{aligned}$$

B.2. Recursive Kernel Learning as Variance Minimization

The proof of Proposition 1 is clear from the main text, but we fill in the missing details here.

Proof of Proposition 1. The only thing left to clarify is the identity

$$tA^{-1}/D = \operatorname{argmax}_{X \succeq 0, \operatorname{tr}(AX) \leq t} \log \det X.$$

Note that $\log \det X$ is strictly convex, and KKT conditions yield that the minimum is a solution to the Lagrangian system of equations. Evaluating, we have

$$L(X, \lambda) = \log \det X - \lambda(\operatorname{tr}(AX) - t) \implies \nabla_X L = X^{-1} - \lambda A = 0.$$

Hence the optimum is proportionate to A^{-1} , and evaluating the constraint yields the result. \square

B.3. Guarantees

To derive the learning rate for the Local EGOP Learning algorithm, we mostly operate at the level of matrices, studying the recurrence from Equation 2. To supplement this in the noisy manifold setting, we rely on critical geometric relations verified in Appendix B.3.2.

B.3.1. SAMPLE TRIMMING

A practical concern when implementing the Local EGOP Learning algorithm is that two points $p, p' \in \mathcal{M}$ may be such that $p - p' \in \mathcal{N}_p$, but $f(p) \neq f(p')$. Such a function can still be continuous index as the line segment between these points goes beyond the reach of the manifold, and thus outside the data sampling region. A simple fix is to exclude data points outside of a fixed isotropic radius of the point of interest x^* , thus trimming the population distribution P . The resulting EGOP matrix will then be defined with respect to an extension outside this domain. We adopt such an extension so that Lemma 17, and the secondary conclusions of Lemma 5, that there is an affine space where the gradient is constant and the Hessian is degenerate, hold globally. Alternatively, one can broach this by taking the covariance cap to 0 at a logarithmic rate, reducing the sampling weight of the non-local region at the expense of a small variance inflation. For simplicity, we adopt the former assumptions.

B.3.2. SUPPORTING ARGUMENTS FOR LEMMA 4

We try to keep our proofs as elementary as possible. We start with basic properties of our function of interest f .

Lemma 13 (Derivatives). *Suppose that $f = f \circ \pi$. Then $\nabla f(x) \in \mathcal{T}_x$ and for any $u, v \in \mathcal{N}_x$, $u^T \nabla^2 f(x)v = 0$.*

Proof. Let $u, v \in \mathcal{N}_x$ be arbitrary. Then,

$$\begin{aligned} \nabla f(x)^T v &= \lim_{t \rightarrow 0} [f(x + tv) - f(x)]/t = \lim_{t \rightarrow 0} [f(\pi[x + tv]) - f(\pi[x])]/t \\ &= \lim_{t \rightarrow 0} [f(\pi[x]) - f(\pi[x])]/t = 0, \end{aligned}$$

as for small t orthogonal perturbations do not change the nearest point on \mathcal{M} . As this holds for generic v the first claim follows. To simplify notation, define $\partial_\eta h(x) := \lim_{t \rightarrow 0} [h(x + t\eta) - h(x)]/t$. We can thus compute

$$u^T \nabla^2 f(x)v = \partial_u(\nabla f^T v)(x) = 0$$

as $\nabla f^T v$ is identically 0 along the path $x + tv$, $t \in [0, \delta]$ for δ small enough. That is, as ∇f remains tangent along this path, as verified above, it is always orthogonal to v . \square

In the interest of further studying the structure of ∇f we verify the following fundamental Geometric facts. We denote by π_V the projection onto the vector space V . Denote by $d(\cdot, \cdot)$ the geodesic distance on \mathcal{M} . Let $\kappa = \sup_{p \in \mathcal{M}, \|v\|=1} \|S_v(p)\|$, S the Weingarten map of \mathcal{M} . This constant is automatically finite as \mathcal{M} has nontrivial reach.

Lemma 14 (Orthogonal Curvature). *There exists a universal constant C such that, for any $p, p^* \in \mathcal{M}$,*

$$\|\pi_{\mathcal{N}_p} - \pi_{\mathcal{N}_{p^*}}\| \leq Cd(p, p^*).$$

Proof. Let $\gamma_t, t \in [0, d(p, p^*)]$ be a unit speed geodesic connecting p and p^* . We can compute

$$\|\pi_{\mathcal{N}_p} - \pi_{\mathcal{N}_{p^*}}\| = \left\| \int_0^1 \partial_t \pi_{\mathcal{N}_{\gamma_t}} dt \right\| \leq \int_0^{d(p, p^*)} \|\partial_t \pi_{\mathcal{N}_{\gamma_t}}\| dt.$$

Thus, if we can show a uniform bound for $\|\partial_t \pi_{\mathcal{N}_{\gamma_t}}\|$ then we are done.

Let v_1, \dots, v_{D-d} be an orthonormal basis of \mathcal{N}_{x^*} , and form the orthonormal moving frame $v_1(t), \dots, v_{D-d}(t)$ along γ_t by parallel translation. Let

$$V(t) := [v_1(t) \quad \dots \quad v_{D-d}(t)].$$

By construction, $\pi_{\mathcal{N}_{\gamma_t}} = V(t)V(t)^T$, $V(t)$ is orthogonal for all t . Differentiating,

$$\|\partial_t \pi_{\mathcal{N}_{\gamma_t}}\| = \|V'(t)V(t)^T + V(t)V'(t)^T\| \leq 2\|V'(t)\|\|V(t)\| = 2\|V'(t)\|.$$

This reduces the problem to uniformly bounding $\|V'(t)\|$. The key relations to prove this are

$$V'(t) = [v'_1(t) \quad \dots \quad v'_{D-d}(t)], \quad v'_i(t) = -S_{v_i(t)}(\gamma_t)\gamma'_t.$$

The first identity is definitional, the second can be found in (Do Carmo, 2016). For $\|u\| = 1$, we have

$$\|V'(t)u\| = \left\| \sum_{i=1}^{D-d} u_i v'_i(t) \right\| = \left\| -S_{\sum_i u_i v_i(t)}(\gamma_t)\gamma'_t \right\| \leq \|S_{\sum_i u_i v_i(t)}(\gamma_t)\gamma'_t\| \leq \kappa,$$

as $\|\sum_i u_i v_i(t)\| \leq \sum_i u_i^2 = 1$, hence $\|V'(t)\| \leq \kappa$ holds uniformly. \square

Lemma 15 (Projection Normal). *For any $v \in \mathcal{N}_{\pi[x]}$, $D\pi_x v = 0$.*

Proof. As computed previously,

$$D\pi_x v = \lim_{t \rightarrow 0} [\pi[x + tv] - \pi[x]]/t = 0.$$

\square

Lemma 16 (Orthogonal Control). *Fix x^* in the tubular neighborhood of \mathcal{M} . There exists $r > 0$ small enough such that, for $\|x - x^*\| \leq r$, there exists a constant $C > 0$ such that*

$$\|\pi_{\mathcal{N}_{x^*}} - \pi_{\mathcal{N}_x}\| \leq C\|\pi_{\mathcal{T}_{x^*}}[x^* - x]\|$$

Proof. By Lemma 14, it suffices to show that $d(\pi[x^*], \pi[x]) = O(\|\pi_{\mathcal{T}_{x^*}}[x^* - x]\|)$. By (Garcia Trillo, 2019), we have that $d(\pi[x^*], \pi[x]) = O(\|\pi[x^*] - \pi[x]\|)$, further reducing the problem. By our locality assumption, we can take convex combinations and remain within the tubular neighborhood, allowing us to decompose

$$\|\pi[x^*] - \pi[x]\| \leq \left\| \int_0^1 D\pi_{x^*+t(x-x^*)}(x - x^*) dt \right\| \leq \int_0^1 \|D\pi_{x^*+t(x-x^*)}(x - x^*)\| dt.$$

By Lemma 15,

$$\begin{aligned} \|D\pi_{x^*+t(x-x^*)}(x - x^*)\| &= \|D\pi_{x^*+t(x-x^*)}(\pi_{\mathcal{T}_{x^*+t(x-x^*)}}[x - x^*])\| \\ &\leq C\|\pi_{\mathcal{T}_{x^*+t(x-x^*)}}[x - x^*]\| \leq C\|[\pi_{\mathcal{T}_{x^*+t(x-x^*)}} - \pi_{x^*}][x - x^*]\| + C\|\pi_{x^*}[x - x^*]\| \\ &\leq Cr\|\pi_{\mathcal{T}_{x^*+t(x-x^*)}} - \pi_{x^*}\| + C\|\pi_{x^*}[x - x^*]\|, \end{aligned}$$

as π is smooth, and we have restricted ourselves to a bounded domain. In other words,

$$\|\pi[x^*] - \pi[x]\| - Cr\|\pi_{\mathcal{T}_{x^*} + t(x-x^*)} - \pi_{\mathcal{T}_{x^*}}\| \leq C\|\pi_{\mathcal{T}_{x^*}}[x - x^*]\|,$$

hence, if we can show that

$$\|\pi_{\mathcal{T}_{x^*} + t(x-x^*)} - \pi_{\mathcal{T}_{x^*}}\| \leq C'\|\pi[x^*] - \pi[x]\|,$$

then for r small enough the desired inequality will be achieved. Notice that $\pi_{\mathcal{T}_x} = I - \pi_{\mathcal{N}_x}$, hence by Lemma 14

$$\|\pi_{\mathcal{T}_{x^*} + t(x-x^*)} - \pi_{\mathcal{T}_{x^*}}\| = \|\pi_{\mathcal{N}_{x^*} + t(x-x^*)} - \pi_{\mathcal{N}_{x^*}}\| \leq \tilde{C}d(\pi[x^*], \pi[x^* + t(x-x^*)]) \leq C'\|\pi[x^*] - \pi[x]\|,$$

completing the proof. \square

We apply this to study ∇f .

Lemma 17 (Gradient Rotation). *Restricting ourselves to a region small enough that Lemma 16 is valid, we have*

$$\|\pi_{\mathcal{N}_{x^*}} \nabla f(x)\| = O(\|\pi_{\mathcal{T}_{x^*}}[x^* - x]\|).$$

Proof. By Lemmas 13 and 16,

$$\|\pi_{\mathcal{N}_{x^*}} \nabla f(x)\| = \|[\pi_{\mathcal{N}_{x^*}} - \pi_{\mathcal{N}_x}] \nabla f(x)\| \leq C\|\pi_{\mathcal{N}_{x^*}} - \pi_{\mathcal{N}_x}\| \leq C'\|\pi_{\mathcal{T}_{x^*}}[x^* - x]\|.$$

\square

B.3.3. SUPPORTING ARGUMENTS FOR LEMMA 5

Lemma 18. *Let $x \in \mathcal{M}$ and $\eta \in \mathcal{N}_x$. Then $D\pi_{x+\eta} = (I - S_x(\eta))^{-1}\pi_{\mathcal{T}_x}$.*

Proof. Clearly, for any normal vector $v \in \mathcal{N}_x$, $D\pi_{x+\eta}v = 0$, as projection is invariant to normal displacement. Thus it suffices to verify the formula for any tangent vector. Our proof has two primary parts. First, we pass to normal coordinates, equating the tubular neighborhood about \mathcal{M} with the normal bundle, and compute the differential of the exponential map. From this parameterization, we can then analyze the projection via the chain rule.

Starting from the normal bundle $N\mathcal{M}$, for $(x, v) \in N_x\mathcal{M}$, the exponential map $E(x, v) = x + v$ is a diffeomorphism to the tube. Let $\gamma(t) = (u(t), \xi(t)) \in N\mathcal{M}$, $\gamma'(t) \in TN\mathcal{M}$. We compute $\xi'(0) = -S_x(v)u'(0) + \nabla_{u'(0)}^\perp \xi(0)$, hence

$$DE_{(x,v)}\gamma'(0) = u + [-S_x(v)u + \nabla_{u'(0)}^\perp \xi(0)] = (I - S_x(v))u + \nabla_{u'(0)}^\perp \xi(0).$$

Composing with the projection map, $\pi \circ E(x, v) = x$, hence

$$D\pi_{x+v}DE_{(x,v)}\gamma'(0) = u'(0) \iff D\pi_{x+v}\pi_{\mathcal{T}_x}[(I - S_x(v))u] = u'(0),$$

and inverting yields the claim, as $D\pi_{x+v}$ is a linear operator. \square

Proof of Lemma 5. The first claim follows immediately from Lemma 18 and the chain rule, indeed,

$$\nabla f(x + v) = \nabla g(\pi(x + v)) = (I - S_x(v))^{-1}\nabla g(x).$$

Let $u = (I - S_x(v))^{-1}\nabla g(x)$. Applying linearity of the shape operator, observe that $(I - S_x(v + \eta))u = (I - S_x(v))u - S_x(\eta)u = \nabla g(x) - S_x(\eta)u$. Hence, if $S_x(\eta)u = 0$ then $u = \nabla f(x + v + \eta)$. Thus, the second claim follows if we can show that there is a $D - 2d$ dimensional subspace Null that annihilates the solution vector u . For $w \in \mathcal{T}_x$,

$$\langle S_x(\eta)u, w \rangle = \langle \mathbb{II}(u, w), \eta \rangle$$

for \mathbb{II} the second fundamental form. This is a bilinear map, and the map defined by fixing the u argument, $\phi_u(w) := \mathbb{II}(u, w)$ is a linear map from $\mathcal{T}_x \rightarrow \mathcal{N}_x$, and thus has image no larger than d . Its complement $\phi_u(\mathcal{T}_x)^\perp$ has dimension at least $\dim(\mathcal{N}_x) - d = D - 2d$, as desired.

This proves the invariance of the gradient along a space of dimension at least $D - 2d$, which immediately implies $\nabla^2 f(x + v + \eta)z = \partial_z \nabla f(x + v) = 0$. \square

B.3.4. TAYLOR EXPANSION

We first provide the generic Taylor expansion, which we then go on to refine for the noisy manifold setting.

Proof of Lemma 3. We start by Taylor expanding the gradient. For a D tuple ξ , as $\partial_\xi \partial_i f = \partial_i \partial_\xi f$, for f sufficiently smooth we can express

$$\partial_i f(x) = \sum_{|\xi| \leq q} \frac{1}{q!} \partial_i [\partial_\xi f](x) \prod_{q_i \in \xi} x_i^{q_i} + O(\|x\|^{q+1}).$$

In particular, we have

$$\partial_i f(x) = \partial_i f(0) + \sum_j \partial_i \partial_j f(0) x_j + \frac{1}{2} \sum_{j,k} \partial_i \partial_j \partial_k f(0) x_j x_k + O(\|x\|^3).$$

Working at the level of the gradient, this yields

$$\nabla f(x) = \nabla f(0) + \nabla^2 f(0)x + T(x, x) + O(\|x\|^3)$$

where T is the bilinear for

$$[T[x, y]]_i = \frac{1}{2} \sum_{j,k} \partial_i \partial_j \partial_k f(0) x_j y_k.$$

We use the first three terms of this Taylor expansion as a starting point. Set $g := \nabla f(0)$, $H := \nabla^2 f(0)$.

The remainder of the Taylor expansion can be exactly expressed as

$$\tilde{R}(x) = \frac{1}{6} \int_0^1 (1-s)^2 \nabla^4 f(sx)[x, x, x] ds, \quad [\nabla^4 f(sx)[x, x, x]]_i := \sum_{j,k,\ell} \partial_i \partial_j \partial_k \partial_\ell f(sx) x_i x_j x_k.$$

Hence, under our uniform boundedness assumption, we have

$$\|T[x, x]\| \leq C\|x\|^2, \quad \|\tilde{R}(x)\| \leq C\|x\|^3$$

for some constant C . Throughout the argument, for convenience we will absorb constants into C if necessary. Hence,

$$\mathcal{L}(\mu) = \int \nabla f \nabla f^T d\mu = gg^T + H\Sigma H + gT(\Sigma)^T + T(\Sigma)g^T + R(\Sigma),$$

for

$$\begin{aligned} T(\Sigma)_i &:= \mathbb{E}_\mu[T(x, x)_i] = \frac{1}{2} \sum_{j,k} \partial_i \partial_j \partial_k f(0) \Sigma_{jk} \\ R(\Sigma) &:= \mathbb{E}_\mu[T[Z, Z]T[Z, Z]^T + HZ\tilde{R}(Z)^T + \tilde{R}(Z)(HZ)^T + \tilde{R}(Z)\tilde{R}(Z)^T]. \end{aligned}$$

That T is continuous and linear in Σ is immediate. For the remainder, we have

$$\begin{aligned} \|R(\Sigma)\| &\leq \mathbb{E}_\mu[\|T[Z, Z]T[Z, Z]^T\| + \|HZ\tilde{R}(Z)^T\| + \|\tilde{R}(Z)(HZ)^T\| + \|\tilde{R}(Z)\tilde{R}(Z)^T\|] \\ &\leq C\mathbb{E}[\|Z\|^4 + \|Z\|^6] \leq C\mathbb{E}_\mu[\text{tr}(\Sigma^2) + \text{tr}(\Sigma)^2] \end{aligned}$$

where we apply Isserlis's Theorem (Isserlis, 1918) which verifies the vanishing of third order terms, and relates the higher moments to the norm of the covariance matrix. Our capped covariance assumption is used to compress all higher order terms to quadratic order. Our proof is completed upon observing

$$\text{tr}(\Sigma^2) = \|\Sigma\|_F^2, \quad \text{tr}(\Sigma)^2 = \left(\sum_i \lambda_i \right)^2 \leq D \sum_i \lambda_i^2 = D\|\Sigma\|_F^2,$$

and in finite dimensions the frobenius and operator norms are equivalent. \square

Proof of Lemma 4. That $\text{rank}(H) \leq 2d$ is immediate from Lemma 13. Indeed, the $\mathcal{N} \times \mathcal{N}$ block of H is completely 0, hence at most d rows and d columns of H in the $\mathcal{T} \oplus \mathcal{N}$ basis have nonzero entries. Let B_r be

We now apply Lemmas 13 and 17 to compute

$$\begin{aligned} \|\pi_{\mathcal{N}} \mathcal{L}(\mu) \pi_{\mathcal{N}}\| &= \left\| \int \pi_{\mathcal{N}} \nabla f \nabla f^T \pi_{\mathcal{N}} d\mu \right\| \leq \int \|\pi_{\mathcal{N}} \nabla f \nabla f^T \pi_{\mathcal{N}}\| d\mu \\ &= \int \|[\pi_{\mathcal{N}} - \pi_{\mathcal{N}_x}] \nabla f(x) \nabla f(x)^T [\pi_{\mathcal{N}} - \pi_{\mathcal{N}_x}]\| d\mu \\ &\leq C \int \|\pi_{\mathcal{N}} - \pi_{\mathcal{N}_x}\|^2 d\mu \leq C \int \|\pi_{\mathcal{T}} x\|^2 d\mu \leq C[\text{tr}([\pi_{\mathcal{T}} \Sigma \pi_{\mathcal{T}}]^2) + \text{tr}(\pi_{\mathcal{T}} \Sigma \pi_{\mathcal{T}})^2] \leq C \|\pi_{\mathcal{T}} \Sigma \pi_{\mathcal{T}}\|_F^2, \end{aligned}$$

where the final bounds from Isserlis's Theorem are similar to Lemma 3. Similarly,

$$\begin{aligned} \|\pi_{\mathcal{T}} \mathcal{L}(\mu) \pi_{\mathcal{N}}\| &\leq \int \|\pi_{\mathcal{T}} \nabla f(x) \nabla f(x)^T [\pi_{\mathcal{N}} - \pi_{\mathcal{N}_x}]\| d\mu \leq C \int \|\pi_{\mathcal{T}} x\| d\mu \\ &\leq C \sqrt{\int \|\pi_{\mathcal{T}} x\|^2 d\mu} = C \|\pi_{\mathcal{T}} \Sigma \pi_{\mathcal{T}}\|_F. \end{aligned}$$

As the operator and Frobenius norms are equivalent the bounds are as desired. \square

Proof of Corollary 1. The basic claim is immediate from Lemma 3, and that the terms stemming from higher order derivatives are uniformly bounded follows from the smoothness assumptions on f . Further, the nullspace of the Hessian and the 0 order expansion being the gradient $g = \nabla f(x^*)$ follow immediately from Lemma 5. \square

B.3.5. MATRIX RECURRENCE

We begin our study of the recurrence in Equation 2 by introducing a reduced form. We analyze this scheme, and then apply it to Local EGOP Learning, leveraging the results of Appendix B.3.2. We divide our focus into two distinct settings, the first mirroring Equation 6 by introducing a constant shift, and the second mirroring Equation 5 a homogeneous equation.

Constant Shift

Let J be an involution, $J = J^T = J^{-1}$. We introduce the recurrence

$$B_{t+1} = h_{t+1} J (G + \beta B_t + (1 - \beta) B_{t-1} + E_t)^{-1} J$$

where E_t is an error term, $\beta \in (0, 1)$, $G \succ 0$, $B_0 = \alpha I$, $h_1 = \alpha^2$, $B_1 = h_1 J (G + B_0)^{-1} J$, $h_{t+1} = t_i r^2$, $r < 1$.

Lemma 19 (Perturbed Shift). *Suppose there exists a uniform constant C such that $\|E_t\| \leq C\alpha$ for all t . Then, for α small enough,*

$$\|B_{t+1}\| = \Theta(h_t).$$

Proof. That α must be small is not necessary, but this will be a typical setting and will help expedite the proof. Let $\alpha < 1$ be small enough that $\|B_t\| \leq \lambda_{\min}(G)/4$, $t = 1, 2$, and $C\alpha \leq \lambda_{\min}(G)/4$. We prove by strong induction that $\|B_{t+1}\| \leq h_{t+1} \frac{2}{\lambda_{\min}(G)}$. The base case is immediate, so we move on to the inductive step. We can simply compute

$$G + \beta B_t + (1 - \beta) B_{t-1} + E_t \succeq G/2.$$

As J is an orthogonal matrix, we have $\|B_{t+1}\| \leq 2h_{t+1}/\lambda_{\min}(G)$ and the claim follows.

With the decay of B_t being settled, it follows that $B_t = h_{t+1} J G^{-1} J + O(h_{t+1}^2 + h_{t+1}\alpha)$, hence, normalizing by h_{t+1} , we have exact convergence to $J G^{-1} J$ in the noiseless setting. \square

Homogeneous

We move on to the recurrence

$$A_{t+1} = h_{t+1} J (\beta A_t + (1 - \beta) A_{t-1} + E_t)^{-1} J$$

where E_t is an error term, J is an involution, $\beta \in (0, 1)$, $G \succ 0$, $B_0 = \alpha I$, $h_1 = \alpha^2$, $B_1 = h_1 J(G + B_0)^{-1} J$, $h_{t+1} = h_t r^2$, $r < 1$.

We start by reducing this iteration scheme to an autonomous equation.

Proposition 2 (Autonomous Recurrence). *Define $c(r, \beta) := \frac{1}{\beta/r + (1-\beta)/r^2}$ and let $X_t := A_t/\sqrt{c(r, \beta)h_t}$, $R_t := \sqrt{c(r, \beta)}E_t/\sqrt{h_{t+1}}$, and $\eta = \frac{\beta/r}{c(r, \beta)}$. Then X_t satisfies the autonomous recurrence*

$$X_{t+1} = J(\eta X_t + (1 - \eta)X_{t-1} + R_t)^{-1} J$$

Proof. We work this out by simple algebra. First, as an intermediate step, introduce $C_t := A_t/\sqrt{h_t}$, $R'_t := E_t/\sqrt{h_{t+1}}$. Then we can write

$$\begin{aligned} A_{t+1} &= h_{t+1} J(\beta A_t + (1 - \beta)A_{t-1} + E_t)^{-1} J \\ &\iff \frac{A_{t+1}}{\sqrt{h_{t+1}}} = J \left(\beta \frac{A_t}{\sqrt{h_{t+1}}} + (1 - \beta) \frac{A_{t-1}}{\sqrt{h_{t+1}}} + \frac{E_t}{\sqrt{h_{t+1}}} \right)^{-1} J \\ &\iff C_{t+1} = J([\beta/r]C_t + [(1 - \beta)/r^2]C_{t-1} + R'_t)^{-1} J \\ &\iff C_{t+1} = c(r, \beta)J(\eta C_t + (1 - \eta)C_{t-1} + R'_t c(r, \beta))^{-1} J \\ &\iff \frac{C_{t+1}}{\sqrt{c(r, \beta)}} = J \left(\eta \frac{C_t}{\sqrt{c(r, \beta)}} + (1 - \eta) \frac{C_{t-1}}{\sqrt{c(r, \beta)}} + R'_t \sqrt{c(r, \beta)} \right) J \\ &\iff X_{t+1} = J(\eta X_t + (1 - \eta)X_{t-1} + R_t)^{-1} J. \end{aligned}$$

□

Thus to study A_t it suffices to study X_t , then multiply by the corresponding factors. Our analysis proceeds as follows. First, leveraging the Thompson metric (Thompson, 1963), we show that, for summable error R_t , the spectrum of X_t stays bounded away from 0 and ∞ . Then, utilizing this bound, we go on to show convergence of X_t . Define the Thompson metric,

$$d_T(A, B) := \log \max\{M(A/B), M(B/A)\}, \quad M(A/B) := \inf\{\gamma > 0 : A \preceq \gamma B\}.$$

Lemma 20 (Spectral Band). *Suppose that $\sum_i \|R_i\| \leq C\alpha$ and $\max\{d_T(X_0, I), d_T(X_1, I)\} = L_0$. Then, for α sufficiently small,*

$$[e^{-L_0} - O(\alpha)]I \preceq X_t \preceq [e^{L_0} + O(\alpha)]I$$

for all i .

Proof. Notice that

$$(1 - \xi_t)[\eta X_t + (1 - \eta)X_{t-1}] \preceq \eta X_t + (1 - \eta)X_{t-1} + R_t \preceq (1 + \xi_t)[\eta X_t + (1 - \eta)X_{t-1}]$$

for $\xi_t := \|[\eta X_t + (1 - \eta)X_{t-1}]^{-1/2} R_t [\eta X_t + (1 - \eta)X_{t-1}]^{-1/2}\|$. It follows that

$$d_T([\eta X_t + (1 - \eta)X_{t-1}] + R_t, [\eta X_t + (1 - \eta)X_{t-1}]) \leq \log \frac{1 + \xi_t}{1 - \xi_t}$$

Hence, if $e^{-L_t} I \preceq X_t, X_{t-1} \preceq e^{L_t} I$, it follows that $\xi_t \leq e^{L_t} \|R_t\|$ and

$$L_{t+1} \leq L_t + \log \frac{1 + \|R_t\|e^{L_t}}{1 - \|R_t\|e^{L_t}} \iff e^{-L_{t+1}} \geq e^{-L_t} \left(\frac{e^{-L_t} - \|R_t\|}{e^{-L_t} + \|R_t\|} \right) \implies e^{-L_{t+1}} \geq e^{-L_t} - 2\|R_t\|.$$

Thus,

$$e^{-L_t} \geq e^{-L_0} - 2 \sum_{i=1}^{\infty} \|R_i\| \geq e^{-L_0}/2$$

choosing α sufficiently small. □

Lemma 21 (Non-Expansive). *Let X_t, X'_t be autonomous homogeneous recurrences of the form of Proposition 2, with common conjugation matrix J . Then*

$$d_T(X_{t+1}, X'_{t+1}) \leq \max\{d_T(X_t, X'_t), d_T(X_{t-1}, X'_{t-1})\} + O(\|R_t\| + \|R'_t\|)$$

Proof. Set $M_t = \eta X_t + (1 - \eta)X_{t-1}$, $M'_t = \eta X'_t + (1 - \eta)X'_{t-1}$. Using the invariance of the Thompson metric to conjugate by orthogonal matrices and invert, we can compute

$$\begin{aligned} d_T(X_{t+1}, X'_{t+1}) &= d_T(\eta X_t + (1 - \eta)X_{t-1} + R_t, \eta X'_t + (1 - \eta)X'_{t-1} + R'_t) \\ &\leq d_T(M_t, M'_t) + d_T(M_t, M_t + R_t) + d_T(M'_t, M'_t + R'_t). \end{aligned}$$

Checking each term,

$$d_T(M_t, M'_t) \leq \max\{d_T(X_t, X'_t), d_T(X_{t-1}, X'_{t-1})\}$$

as averaging in the Thompson metric is non-expansive.

$$d_T(A, A + A) = \|\log A^{-1/2}(A + E)A^{-1/2}\| = \|\log(I + A^{-1/2}EA^{-1/2})\| = O(\|E\|)$$

for A with non-vanishing spectrum. Lemma 20 verifies that the sequences X_t, X'_t do not degenerate for α sufficiently small, thus showing the claim. \square

Lemma 22 (Definite Hessian). *Let $J = I$. Then for α sufficiently small, $X_t \rightarrow I$.*

Proof. Define $T(x, y) = ((\eta x + (1 - \eta)y)^{-1}, x)$, hence $T(X_t, X_{t-1}) = (X_{t+1}, X_t)$. Define

$$V(x, y) = \max\{d_T(x, I), d_T(y, I)\} = \max\{|\log \lambda_{\max}(x)|, |\log \lambda_{\max}(y)|, |\log \lambda_{\min}(x)|, |\log \lambda_{\min}(y)|\}.$$

Notice that

$$\min\{\lambda_{\min}(x), \lambda_{\min}(y)\} \leq \lambda_{\min}(\eta x + (1 - \eta)y)^{-1} \leq \lambda_{\max}(\eta x + (1 - \eta)y)^{-1} \leq \max\{\lambda_{\max}(x), \lambda_{\max}(y)\}$$

hence $V(T(X_t, X_{t-1})) \leq V(X_t, X_{t-1})$. Thus the noiseless recurrence is autonomous, and the discrete Lasalle invariance principle [Mei & Bullo \(2017, Theorem 2\)](#) yields the existence of a set E_c , $T(E_c) \subseteq E_c$ such that for all $(X, Y) \in E_c$, $V(E_c) = c$ and $\lim_{t \rightarrow \infty} \inf_{E \in E_c} \|(X_t, X_{t-1}) - E\| \rightarrow 0$. To verify that $X_t \rightarrow I$ in the noiseless case, it suffices to show $E_0 = \{(I, I)\}$ is the only invariant set with constant value function.

We argue by contradiction. Let E_c be such a limit set, $c > 0$. Take $(X_1, X_0) \in E_c$, and consider $(X_3, X_2) = T^2(X_1, X_0)$. By the condition on the value function V , either the largest eigenvalue of these matrices is e^c or the smallest is e^{-c} . Without loss of generality, assume that X_3 achieves the eigenvalue e^c .

For this to occur, it must be that both X_2, X_1 have eigenvalue e^{-c} with a common eigenvector v . As the sequence is rational in X_2, X_1 , v will be an eigenvector for all subsequent matrices X_t . Notice $\log \lambda_v(X_4) = -\log(\eta e^c + (1 - \eta)e^{-c}) \in (-c, c)$, hence $\sup_{t > 0} |\log \lambda_v(X_{3+t})| < c$, and this eigenspace can never again be extremal. Indeed, for $\lambda_v(X_{3+t}) = e^{\pm c}$, we require $\lambda_v(X_{2+t}) = \lambda_v(X_{1+t}) = e^{\mp c}$, thus any extremal eigenspace for $T^2(X_1, X_0)$ will decay upon further iterations, and non-extremal eigenspaces cannot become extremal. In particular, $V(T^k(X_1, X_0))$ must decrease as $k \rightarrow \infty$, contradicting that E_c is invariant with fixed value function $V(E) = c$ for all $E \in E_c$.

In the noisy setting, Lemma 20 verifies that the recurrence remains compact for α sufficiently small. Hence, we can apply [Mischaikow et al. \(1995, Theorem 1.8\)](#) to verify that the perturbed recurrence converges to the same limit sets as the autonomous recurrence, i.e. I is the unique limit point. \square

Lemma 23 (Generic J). *Suppose that J has signature (k, j) . Then, for α sufficiently small, $X_i \rightarrow L \in \{X : (XJ)^2 = I\}$. Further, L has at most $2 \min\{k, j\}$ eigenvalues not equal to 1.*

Proof. We update the recurrence in Lemma 22 by J congruence. V is still monotone in the autonomous noiseless recurrence as J is orthogonal. We begin by investigating the structure of any invariant set E_c .

As in the previous proof, if we initialize with a pair in E_c , then for any $t \geq 2$, and all extremal eigenpairs (λ_ℓ, v_ℓ) , it must be that for both $j = t - 1, t - 2$, the matrices X_j have matching eigenpairs $(1/\lambda_\ell, Jv_\ell)$. Repeating this argument for

X_{t+1} , for any extremal eigenpairs (ν_ℓ, u_ℓ) it follows that X_t, X_{t-1} have matching eigenpairs $(1/\nu_\ell, Ju_\ell)$. Combining this information, for each extremal eigenpair (ν_ℓ, u_ℓ) of X_{t+1} , $(1/\nu_\ell, Ju_\ell)$ must be an eigenpair of both X_t and X_{t-1} . As $(\lambda_\ell, v_\ell) = (1/\nu_\ell, Ju_\ell)$ is an extremal eigenpair of X_t , it must also be that (ν_ℓ, u_ℓ) is an eigenpair of X_{t-1} . Hence the matrix X_{t-1} has both $(1/\nu_\ell, Ju_\ell)$ and (ν_ℓ, u_ℓ) as extremal eigenpairs, and for them to pass forward in the recurrence they must be shared by X_{t-1} . Thus we see that for all $m \geq t$, $(1/\nu_\ell, Ju_\ell)$ and (ν_ℓ, u_ℓ) are fixed eigenvectors of X_m .

Thus we have proven that any limiting set in E_c has fixed, cyclical extremal eigenpairs. Suppose that X_t has κ such limiting maximal eigenvalues. Let $\text{Trunc}_\kappa(X)$ be the map that identifies X with the $(D - \kappa) \times (D - \kappa)$ matrix formed by removing the principal κ components. Thus, $\text{Trunc}_\kappa T(X_{t+1}, X_t) = T(\text{Trunc}_\kappa(X_t, X_{t-1})) + o(1)$, and the sequence $\text{Trunc}_\kappa(X_t, X_{t-1})$ is asymptotically autonomous and monotone in the value function V . Hence Mischaikow et al. (1995, Theorem 1.8) yields that the truncated sequence has asymptotically cyclical extremal eigenvectors.

Inductively applying this argument verifies that $X_t \rightarrow L$ for a fixed matrix L in the noiseless case. By definition

$$L = \lim_{t \rightarrow \infty} X_{t+1} = \lim_{t \rightarrow \infty} J(\eta X_{t+1} + (1 - \eta)X_t)^{-1}J = JL^{-1}J,$$

hence $L \in \{X : (LJ)^2 = I\}$. In the perturbed setting, Lemma 20 verifies that the recurrence remains compact for α sufficiently small. Hence, we can once again apply Mischaikow et al. (1995, Theorem 1.8) to verify that the recurrence converges to the same limit sets as the autonomous recurrence.

We now study the structure of such L . As we demonstrated, every eigenpair (λ, v) of L must have matching eigenpair $(1/\lambda, Jv)$. Let $v_1, \dots, v_\kappa, Jv_1, \dots, Jv_\kappa, u_1, \dots, u_{D-2\kappa}$, where $Ju_i = \pm u_i$ are invariant under J . Displaying J in this basis, we have

$$J = \begin{bmatrix} 0 & I & 0 \\ I & 0 & 0 \\ 0 & 0 & D \end{bmatrix}$$

The first $2\kappa \times 2\kappa$ block has signature (κ, κ) , yielding the desired claim. \square

Lemma 24 (Commuting Seeds). *Let $r \in (0, 1)$, $\|R_t\| \leq C\alpha r^t$, X_0, X_1 commute with J . Then, for any $\varepsilon > 0$, there exists $\delta > 0$ such that $X_t \rightarrow L_\alpha$, $\|L_\alpha - I\| < \varepsilon$.*

Proof. That X_t has a limit L_α for α small follows immediately from Lemma 23. Thus it suffices to verify that $\lim_{t \rightarrow \infty} X_t = I$ for the unperturbed sequence. Indeed, if for t large enough, $\|X_t - I\| < \varepsilon$, $\|X_{t-1} - I\| < \varepsilon$, because X_t is rational in X_0, X_1, R_j , $j = 1, \dots, i-1$, it follows that it is smooth for α small, thus incurring additional $O(\alpha)$ error. In combination with Lemma 20, this verifies the claim.

Without perturbations, the whole sequence commutes, and

$$J(\eta X_t + (1 - \eta)X_{t-1})^{-1}J = (\eta X_t + (1 - \eta)X_{t-1})^{-1}J^2 = (\eta X_t + (1 - \eta)X_{t-1})^{-1}$$

hence J factors out, and the convergence is a consequence of Lemma 22. \square

B.3.6. FULL RANK HESSIAN

Our main proof strategy is to reduce the Local EGOP iterations to the form of Proposition 2, so that we can guarantee stable first and second order convergence rates by Lemmas 19 and 23. Let H have diagonalization $H = U\Lambda U^T$. A straightforward change of variables yields the following.

Proposition 3 (H Reduction). *Let $J = \text{sign}(\Lambda)$ be the diagonal signature matrix and $W = U|\Lambda|^{1/2}$.*

Define the transformation

$$X_t := W^T \Sigma_t W, \quad \tilde{g} := JW^{-1}g, \\ \tilde{T}(X) := JW^{-1}T(W^{-T}XW^{-1})W^{-T}J, \quad \tilde{R}(X) := JW^{-1}R(W^{-T}XW^{-1})W^{-T}J.$$

Then the recurrence for X_t depends only on J :

$$\begin{aligned} X_{t+1} = t_{t+1} J & \left(\tilde{g} \tilde{g}^T + \beta X_t + (1 - \beta) X_{t-1} \right. \\ & + \beta [\tilde{g} \tilde{T}(X_t)^T + \tilde{T}(X_t) \tilde{g}^T + \tilde{R}(X_t)] \\ & \left. + (1 - \beta) [\tilde{g} \tilde{T}(X_{t-1})^T + \tilde{T}(X_{t-1}) \tilde{g}^T + \tilde{R}(X_{t-1})] \right)^{-1} J \end{aligned}$$

Thus we can reduce our recurrence to that studied in Section B.3.5.

Lemma 25 (Schur Complement). Define $u := g/\|g\|$, $\bar{\pi} := uu^T$, $\bar{Q} := I - \bar{\pi}$, $H_{\bar{Q}} = \bar{Q}H\bar{Q}$. Let

$$\begin{aligned} \alpha_t &:= u^T \Sigma_t u, \quad \alpha'_t := u^T H \Sigma_t H u, \quad \eta^2 := \|g\|^2, \quad b_t := \bar{Q} \Sigma_t u, \quad b'_t := \bar{Q} H \Sigma_t H u, \\ C_t &:= \bar{Q} \Sigma_t \bar{Q}, \quad C'_t := \bar{Q} H \Sigma_t H \bar{Q}, \quad R_{b,t} := \eta \bar{Q} T(\Sigma_t) + \bar{Q} R(\Sigma_t) u, \\ \bar{R}_{\alpha,t} &:= \beta [2\eta u^T T(\Sigma_t) + u^T R(\Sigma_t) u] + (1 - \beta) [2\eta u^T T(\Sigma_{t-1}) + u^T R(\Sigma_{t-1}) u], \\ \bar{b}_t &= \beta [b'_t + R_{b,t}] + (1 - \beta) [b'_{t-1} + R_{b,t-1}], \quad \bar{R}_{C,t} := \beta \bar{Q} R(\Sigma_t) \bar{Q} + (1 - \beta) \bar{Q} R(\Sigma_{t-1}) \bar{Q}, \\ \bar{S}_t &:= \beta H_{\bar{Q}} C_t H_{\bar{Q}} + (1 - \beta) H_{\bar{Q}} C_{t-1} H_{\bar{Q}} + \bar{R}_{C,t} - \frac{1}{\eta^2 + \alpha_t + \bar{R}_{\alpha,t}} \bar{b}_t \bar{b}_t^T. \end{aligned}$$

Then, in the orthonormal basis $\{u\} \oplus \text{range}(\bar{Q})$,

$$\begin{bmatrix} \alpha_{t+1} & b_{t+1}^T \\ b_{t+1} & C_{t+1} \end{bmatrix} = t_{t+1} \begin{bmatrix} \frac{1}{\eta^2 + \alpha'_t + \bar{R}_{\alpha,t}} + \left(\frac{1}{\eta^2 + \alpha'_t + \bar{R}_{\alpha,t}} \right)^2 \bar{b}_t^T \bar{S}_t^{-1} \bar{b}_t & -\frac{1}{\eta^2 + \alpha'_t + \bar{R}_{\alpha,t}} \bar{b}_t^T \bar{S}_t^{-1} \\ -\bar{S}_t^{-1} \bar{b}_t \frac{1}{\eta^2 + \alpha'_t + \bar{R}_{\alpha,t}} & \left(\beta C'_t + (1 - \beta) C'_{t-1} + \bar{R}_{C,t} - \frac{1}{\eta^2 + \alpha_t + \bar{R}_{\alpha,t}} \bar{b}_t \bar{b}_t^T \right)^{-1} \end{bmatrix}.$$

Proof. This is the Schur complement with pivot on the top-left scalar applied to $M_t := [\beta \mathcal{L}(\mu_t) + (1 - \beta) \mathcal{L}(\mu_{t-1})]^{-1}$. \square

Corollary 3 (Base Case). Suppose that $\Sigma_0 = \alpha I$ and $t_1 = \alpha^2$. Then, in the (u, \bar{Q}) basis,

$$\Sigma_1 = \begin{bmatrix} \frac{\alpha^2}{\eta^2} + O(\alpha^3) & O(\alpha^2) \\ O(\alpha^2) & \alpha(\bar{Q} H^2 \bar{Q})^{-1} + O(\alpha^2) \end{bmatrix}, \quad \Sigma_2 = \begin{bmatrix} \frac{\alpha^2}{\eta^2} + O(\alpha^3) & O(\alpha^2) \\ O(\alpha^2) & \alpha H_{\bar{Q}}^{-1} H^2 H_{\bar{Q}}^{-1} + O(\alpha^2) \end{bmatrix}$$

Proof. This can be directly computed from the formula in Lemma 25. As a subtle detail, at the first step, the covariance is isotropic, hence in the $\bar{Q} \times \bar{Q}$ block the dominant terms is $\alpha(\bar{Q} H(I) H \bar{Q})^{-1} = \alpha(\bar{Q} H^2 \bar{Q})^{-1}$, however, after this step the gradient element of the covariance is a higher order residual, being of the Lemma 19 constant shift form, and thus subsequently $\bar{Q} H \Sigma_1 H \bar{Q} = (\bar{Q} H \bar{Q}) \Sigma_1 (\bar{Q} \Sigma_1 \bar{Q}) + O(\alpha^2) =: H_{\bar{Q}} \Sigma_1 H_{\bar{Q}} + O(\alpha^2)$. \square

Proof of Theorem 1. We seek to inductively apply Lemmas 19 and 24 to the $u \times u$ and $\bar{Q} \times \bar{Q}$ blocks respectively, necessitating a careful tabulation of the residuals and off-diagonals. Our inductive hypothesis is that

$$\alpha_t = \Theta(h_t), \quad b_t = O(\sqrt{h_t}), \quad C_t = \Theta(\sqrt{h_t}), \quad \bar{R}_{C,t} = O(h_t), \quad \bar{R}_{b,t} = O(\sqrt{h_t}), \quad \bar{R}_{\alpha,t} = O(\sqrt{h_t}).$$

We argue by strong induction, with the base case being covered in Corollary 3. We argue one block at a time. First note that $\bar{b}_t^T \bar{S}_t^{-1} \bar{b}_t = O(\sqrt{h_t})$, hence

$$\frac{1}{\eta^2 + \alpha'_t + \bar{R}_{\alpha,t}} + \left(\frac{1}{\eta^2 + \alpha'_t + \bar{R}_{\alpha,t}} \right)^2 \bar{b}_t^T \bar{S}_t^{-1} \bar{b}_t = \frac{1}{\eta^2} + O(\sqrt{h_t}) \implies \alpha_{t+1} = \frac{h_{t+1}}{\eta^2} + O(h_{t+1}^{3/2}).$$

Thus, taking α sufficiently small, we get a uniform $O(h_t)$ bound by Lemma 19 and Proposition 3.

For the $\bar{Q} \times \bar{Q}$ block,

$$C_{t+1} = h_{t+1} \left(\beta H_{\bar{Q}} C_t H_{\bar{Q}} + (1 - \beta) H_{\bar{Q}} C_{t-1} H_{\bar{Q}} + \left[\bar{Q} H \bar{\pi} (\beta \Sigma_t + (1 - \beta) \Sigma_{t-1}) \bar{\pi} H \bar{Q} + \bar{R}_{C,t} - \frac{1}{\eta^2 + \alpha_t + \bar{R}_{\alpha,t}} \bar{b}_t \bar{b}_t^T \right] \right)^{-1}.$$

As the rescaled residual

$$\left[\bar{Q}H\bar{\pi}(\beta\Sigma_t + (1-\beta)\Sigma_{t-1})\bar{\pi}H\bar{Q} + \bar{R}_{C,t} - \frac{1}{\eta^2 + \alpha_t + \bar{R}_{\alpha,t}}\bar{b}_t\bar{b}_t^T \right] / \sqrt{h_t} \leq C\sqrt{h_t} = C\alpha r^t$$

is uniformly summable in α , we can apply Propositions 2 and 3, and Lemma 23 to verify $C_{t+1} = \Theta(\sqrt{h_t})$.

Moving on to the off-diagonal, $-\frac{1}{\eta^2 + \alpha_t + \bar{R}_{\alpha,t}}\bar{b}_t^T\bar{S}_t^{-1} = O(1)$, thus upon multiplying by h_{t+1} , this is $O(h_t)$, whereas the subsequent remainder terms $R_{b,t+1} = \Theta(\|\Sigma_{t+1}\|) = O(\sqrt{h_{t+1}})$. Thus, the contribution is negligible at the following iteration, and the uniform rate follows.

We can immediately plug these rates into our risk bounds to yield $\sqrt{\det \Sigma_t} = \Theta(h_t^{(D+1)/4})$, $W(\mu_t) = O(h_t)$, thus yielding the desired rate. \square

B.3.7. NOISY MANIFOLD

We start off by iterating Corollary 1 as described in the text. Let $\Sigma_{\text{Null}^\perp} := \pi_{\text{Null}^\perp}\Sigma\pi_{\text{Null}^\perp}$, $\Sigma_{\text{Null}} := \pi_{\text{Null}}\Sigma\pi_{\text{Null}}$.

Lemma 26 (Weak Dependence). *Suppose that for all $v \in \text{Null}$, $\eta \in \text{Null}^\perp$, $\eta^T\Sigma v = O(\|\Sigma_{\text{Null}^\perp}\|)$, and $\Sigma_{\text{Null}} = \Theta(1)$. There exists $H_{\Sigma_{\text{Null}}}, T_{\Sigma_{\text{Null}}}$ such that*

$$\mathcal{L}(\mu) = gg^T + H_{\Sigma_{\text{Null}}}\Sigma_{\text{Null}^\perp}H_{\Sigma_{\text{Null}}} + gT_{\Sigma_{\text{Null}}}(\Sigma_{\text{Null}^\perp})^T + T_{\Sigma_{\text{Null}}}(\Sigma_{\text{Null}^\perp})g^T + R_{\Sigma_{\text{Null}}}(\Sigma_{\text{Null}^\perp}),$$

$$\|T_{\Sigma_{\text{Null}}}(\Sigma_{\text{Null}^\perp})\| = O(\|\Sigma_{\text{Null}^\perp}\|), \|R_{\Sigma_{\text{Null}}}(\Sigma_{\text{Null}^\perp})\| = O(\|\Sigma_{\text{Null}^\perp}\|^2).$$

Proof. Applying our Gaussian ansatz,

$$\Sigma_v := \text{Cov}_{N(x^*, \Sigma)}(X | \pi_{\text{Null}}[X - x^*] = v) = \Sigma_{\text{Null}^\perp} - [\pi_{\text{Null}^\perp}\Sigma\pi_{\text{Null}}]\Sigma_{\text{Null}}^{-1}[\pi_{\text{Null}}\Sigma\pi_{\text{Null}^\perp}] = \Sigma_{\text{Null}^\perp} + O(\|\Sigma_{\text{Null}^\perp}\|^2).$$

Thus, by Corollary 1,

$$\begin{aligned} \mathcal{L}(\mu_v) &= gg^T + H_v\Sigma_vH_v + gT_v(\Sigma_v)^T + T_v(\Sigma_v)g^T + R_v(\Sigma_v) \\ &= gg^T + H_v\Sigma_{\text{Null}^\perp}H_v + gT_v(\Sigma_{\text{Null}^\perp})^T + T_v(\Sigma_{\text{Null}^\perp})g^T + R_v(\Sigma_{\text{Null}^\perp}) + O(\|\Sigma_{\text{Null}^\perp}\|^2), \end{aligned}$$

and this latter term can be absorbed into the remainder. Now, integrating out v the relevant operators are

$$H_{\Sigma_{\text{Null}}} = \int H_{\pi_{\text{Null}}[x-x^*]} d\mu(x), \quad T_{\Sigma_{\text{Null}}} = \int T_{\pi_{\text{Null}}[x-x^*]} d\mu(x), \quad R_{\Sigma_{\text{Null}}} = \int R_{\pi_{\text{Null}}[x-x^*]} d\mu(x).$$

\square

While this matrix depends on the Null component of Σ , we will develop a recurrence where this is consistent across iterations. We now expand Lemma 25 in the low-rank Hessian setting.

Lemma 27 (Low-rank Schur). *For $\Sigma = \alpha I$ operators are defined as in Lemma 25, otherwise their equivalents as introduced in Lemma 26. Decomposing in the $(\bar{Q}_{\text{Null}^\perp}, \bar{Q}_{\text{Null}}) := (\text{col}(\bar{Q}) \cap \text{Null}^\perp, \text{col}(\bar{Q}) \cap \text{Null})$ basis, let*

$$\begin{aligned} \tilde{R}_{C,t} &:= \bar{R}_{C,t} - \frac{1}{\eta^2 + \alpha_t + \bar{R}_{\alpha,t}}\bar{b}_t\bar{b}_t^T, \quad \bar{C}_t := \beta C'_t + (1-\beta)C'_t, \quad A_t = \bar{Q}_{\text{Null}^\perp}\bar{C}_t\bar{Q}_{\text{Null}^\perp} + \bar{Q}_{\text{Null}^\perp}\tilde{R}_{C,t}\bar{Q}_{\text{Null}^\perp}, \\ W_t &= \bar{Q}_{\text{Null}}\tilde{R}_{C,t}\bar{Q}_{\text{Null}} - \bar{Q}_{\text{Null}}\tilde{R}_{C,t}\bar{Q}_{\text{Null}^\perp}[\bar{Q}_{\text{Null}^\perp}\bar{C}_t\bar{Q}_{\text{Null}^\perp}]^{-1}\bar{Q}_{\text{Null}^\perp}\tilde{R}_{C,t}\bar{Q}_{\text{Null}}. \end{aligned}$$

$$C_{t+1} = h_{t+1} \begin{bmatrix} A_t^{-1} + A_t^{-1}[\bar{Q}_{\text{Null}^\perp}\tilde{R}_{C,t}\bar{Q}_{\text{Null}}]W_t^{-1}[\bar{Q}_{\text{Null}}\tilde{R}_{C,t}\bar{Q}_{\text{Null}^\perp}]A_t^{-1} & -A_t^{-1}\bar{Q}_{\text{Null}^\perp}\tilde{R}_{C,t}\bar{Q}_{\text{Null}}W_t^{-1} \\ -W_t^{-1}\bar{Q}_{\text{Null}}\tilde{R}_{C,t}\bar{Q}_{\text{Null}^\perp}A_t^{-1} & W_t^{-1} \end{bmatrix}$$

Proof. Recall that $C_{t+1} := t_{t+1}(\bar{C}_t + \tilde{R}_{C,t})^{-1}$, hence this is the block Schur complement in the specified basis pivoted on the $\bar{Q}_{\text{Null}^\perp} \times \bar{Q}_{\text{Null}^\perp}$ block. \square

Corollary 4 (\bar{Q} block). Suppose that $\Sigma_0 = \alpha I$ and $t_1 = \alpha^2$. Then, in the $(\bar{Q}_{\text{Null}^\perp}, \bar{Q}_{\text{Null}})$ basis

$$C_1 = \begin{bmatrix} \alpha(\bar{Q}_{\text{Null}^\perp} H^2 \bar{Q}_{\text{Null}^\perp})^{-1} + O(\alpha^2) & O(\alpha) \\ O(\alpha) & \alpha^2 [\bar{Q}_{\text{Null}} \tilde{R}_{C,0} \bar{Q}_{\text{Null}}]^{-1} + O(\alpha) \end{bmatrix},$$

$$C_2 = \begin{bmatrix} \alpha H_{\bar{Q}_{\text{Null}^\perp}}^{-1} H^2 H_{\bar{Q}_{\text{Null}^\perp}}^{-1} + O(\alpha^2) & O(\alpha) \\ O(\alpha) & \alpha^2 [\bar{Q}_{\text{Null}} \tilde{R}_{C,1} \bar{Q}_{\text{Null}}]^{-1} + O(\alpha) \end{bmatrix}.$$

The matrix $\alpha^2 [\bar{Q}_{\text{Null}} \tilde{R}_{C,t} \bar{Q}_{\text{Null}}]^{-1} = \Theta(1)$, $t = 0, 1$.

Proof. We can once again check this via direct computation utilizing Lemma 27. As \bar{C}_0 comprises terms linear in Σ_0 , it is $\Theta(\alpha)$, meanwhile the remainder terms $\tilde{R}_{C,0} = O(\alpha^2)$. Hence $A_0 = \bar{Q}_{\text{Null}^\perp} \bar{C}_0 \bar{Q}_{\text{Null}^\perp} + O(\alpha^2)$, $W_i = \bar{Q}_{\text{Null}} \tilde{R}_{C,0} \bar{Q}_{\text{Null}} + O(\alpha^3)$, and the remaining approximations directly follow. As in the proof of Lemma 3, at the first step, the covariance is isotropic, hence in the $\bar{Q}_{\text{Null}^\perp} \times \bar{Q}_{\text{Null}^\perp}$ block the dominant terms is $\alpha(\bar{Q}_{\text{Null}^\perp} H(I) H \bar{Q}_{\text{Null}^\perp})^{-1} = \alpha(\bar{Q}_{\text{Null}^\perp} H^2 \bar{Q}_{\text{Null}^\perp})^{-1}$, however, after this step the gradient element of the covariance is a higher order residual, being of the Lemma 19 constant shift form, and thus subsequently $\bar{Q}_{\text{Null}^\perp} H \Sigma_1 H \bar{Q}_{\text{Null}^\perp} = (\bar{Q}_{\text{Null}^\perp} H \bar{Q}_{\text{Null}^\perp}) \Sigma_1 (\bar{Q}_{\text{Null}^\perp} H \bar{Q}_{\text{Null}^\perp}) + O(\alpha^2) =: H_{\bar{Q}_{\text{Null}^\perp}} \Sigma_1 H_{\bar{Q}_{\text{Null}^\perp}} + O(\alpha^2)$. \square

Corollary 5 (Noisy Manifold Base Case). Suppose that $X_0 = \alpha I$ and $h_1 = \alpha^2$. In the basis $(g, \bar{Q}_{\text{Null}^\perp}, \bar{Q}_{\text{Null}})$, we have

$$\Sigma_1 = \begin{bmatrix} \frac{\alpha^2}{\eta^2} + O(\alpha^3) & O(\alpha^2) & O(\alpha) \\ O(\alpha^2) & \alpha(\bar{Q}_{\text{Null}^\perp} H^2 \bar{Q}_{\text{Null}^\perp})^{-1} + O(\alpha^2) & O(\alpha) \\ O(\alpha) & O(\alpha) & \Theta(1) \end{bmatrix},$$

$$\Sigma_2 = \begin{bmatrix} \frac{\alpha^2}{\eta^2} + O(\alpha^3) & O(\alpha^2) & O(\alpha) \\ O(\alpha^2) & \alpha H_{\bar{Q}_{\text{Null}^\perp}}^{-1} H^2 H_{\bar{Q}_{\text{Null}^\perp}}^{-1} + O(\alpha^2) & O(\alpha) \\ O(\alpha) & O(\alpha) & \Theta(1) \end{bmatrix}.$$

Proof. Corollary 4 accounts for the bottom right 2×2 block, what remains is to verify the top and left rows. Specifically, we must verify how

$$C_1(b_0 + R_{b,0}) := \alpha^2 \left(\alpha H_{\bar{Q}}^2 + \bar{R}_{C,0} - \frac{1}{\eta^2 + \alpha_0 + \bar{R}_{\alpha,0}} \bar{b}_0 \bar{b}_0^T \right)^{-1} (b_0 + R_{b,0})$$

decomposes across $\bar{Q}_{\text{Null}^\perp}, \bar{Q}_{\text{Null}}$. Applying Corollary 4, we can express this block-wise as

$$\begin{bmatrix} O(\alpha^2) \\ O(\alpha) \end{bmatrix} = \begin{bmatrix} O(\alpha) & O(\alpha) \\ O(\alpha) & O(1) \end{bmatrix} \begin{bmatrix} O(\alpha) \\ O(\alpha) \end{bmatrix}$$

yielding the desired rates. The proof for Σ_2 is essentially the same. \square

Define $\mu(\zeta) = N(x^*, [\Sigma - \Sigma_{\text{Null}^\perp}] + \zeta \bar{Q}_{\text{Null}})$, i.e. the distribution with Null \times Null component fixed to ζ .

Lemma 28 (Filtered Null). Assume that $D \geq 2d$ and $\text{rank}(H) = 2d$. Let

$$\Sigma_{t+1} = t_{t+1} [\beta \mathcal{L}(\mu_t(\zeta)) + (1 - \beta) \mathcal{L}(\mu_{t-1}(\zeta))]^{-1}$$

$\sqrt{t_t} = \alpha r^t$, $0 < r < 1$, $\beta > 0$. Then, for α, ζ sufficiently small, $g^T \Sigma_t g = \Theta(h_t)$, for $v \in \text{Null}$, $v^T \Sigma_t v = \Theta(1)$, and for $\eta \in \text{Null}^\perp \cap g^\perp$, $\eta^T \Sigma \eta = \theta(\sqrt{h_t})$.

Proof. Applying Corollary 1, we can express

$$\mathcal{L}(\mu) = \int \mathcal{L}(\mu_v) d\nu(v) = \int H_v \Sigma_v H_v + g T_v (\Sigma_v)^T + T(\Sigma_v)^T + R_v(\Sigma_v) d\nu(v),$$

where ν is the marginal density $\nu(v) = p_\mu(\pi_{\text{Null}}[X - x^*] = v)$.

We can apply Corollary 5 to verify that the desired anisotropy is present starting from an isotropic initialization. We first study the modified recurrence where the metric M is in terms of $\mathcal{L}'(\mu)$ rather than the EGOP. We proceed by induction to verify that these rates are maintained. Our inductive hypothesis is that

$$\begin{aligned}\alpha_t &= \Theta(h_t), & b_t &= O(\sqrt{h_t}), & C_t &= \Theta(\sqrt{h_t}), & \bar{R}_{C,t} &= O(h_t), \\ \bar{R}_{b,t} &= O(\sqrt{h_t}), & \bar{R}_{\alpha,t} &= O(\sqrt{h_t}), & \|\bar{Q}_{\text{Null}^\perp} \Sigma_t \bar{Q}_{\text{Null}}\| &= O(\sqrt{h_t}).\end{aligned}$$

The weak Null, Null^\perp correlation allows us to apply Lemma 26 to reduce the recurrence to the marginal form

$$\mathcal{L}(\mu_\zeta) = gg^T + H_\zeta \Sigma_{\text{Null}^\perp} H_\zeta + gT_\zeta(\Sigma_{\text{Null}^\perp})^T + T_\zeta(\Sigma_{\text{Null}^\perp})g^T + R_\zeta(\Sigma_{\text{Null}^\perp}).$$

By assumption $H_0 = H$ is maximal rank, hence for ζ sufficiently small this property is maintained for H_ζ , and we restrict our analysis to this neighborhood. The verification for the $g \times g$ block is exactly the same as verified in Theorem 1 as it is of constant shift form (see Lemma 19), thus we move on to the remaining terms. Explicit computations are similar to those previously presented in Corollaries 4 and 5. First, we immediately have that

$$A_t = H_{\bar{Q}_{\text{Null}^\perp}} [\beta C_t + (1 - \beta) C_{t-1}] H_{\bar{Q}_{\text{Null}^\perp}} + O(h_t), \quad W_t = \bar{Q}_{\text{Null}} \tilde{R}_{C,t} \bar{Q}_{\text{Null}} + O(h_t^{3/2}).$$

Thus for the middle block, applying Lemma 27 yields

$$\bar{Q}_{\text{Null}^\perp} C_{t+1} \bar{Q}_{\text{Null}^\perp} = t_{t+1} \{ H_{\bar{Q}_{\text{Null}^\perp}} [\beta(\bar{Q}_{\text{Null}^\perp} C_t \bar{Q}_{\text{Null}^\perp}) + (1 - \beta)(\bar{Q}_{\text{Null}^\perp} C_{t-1} \bar{Q}_{\text{Null}^\perp})] H_{\bar{Q}_{\text{Null}^\perp}} + O(h_t) \}^{-1}.$$

by the reductions from Propositions 2 and 3, we can reduce this to an autonomous recurrence in $\bar{Q}_{\text{Null}^\perp} C_t \bar{Q}_{\text{Null}^\perp}$ that converges at the desired rate by Lemma 23. See the proof of Theorem 1 for more details.

Applying Lemma 27 again yields

$$\bar{Q}_{\text{Null}} C_{t+1} \bar{Q}_{\text{Null}} = h_{t+1} W_t^{-1} = h_{t+1} (\bar{Q}_{\text{Null}} \tilde{R}_{C,t} \bar{Q}_{\text{Null}})^{-1} + O(\sqrt{h_t}).$$

As $\bar{Q}_{\text{Null}} \tilde{R}_{C,t} \bar{Q}_{\text{Null}} = O(\|\Sigma_{\text{Null}^\perp}\|^2) = O(h_t)$, it follows that $h_{t+1} (\bar{Q}_{\text{Null}} \tilde{R}_{C,t} \bar{Q}_{\text{Null}})^{-1} = \Omega(1)$, and thus it is of constant order by our covariance cap. Thus this rate is an immediate consequence of the second order anisotropy, and the orthogonal component and other remainders only contribute negligibly, justifying the uniform rate. The remaining terms in the Lemma 27 block decomposition are

$$\bar{Q}_{\text{Null}^\perp} \Sigma_{t+1} \bar{Q}_{\text{Null}} = \bar{Q}_{\text{Null}^\perp} C_{t+1} \bar{Q}_{\text{Null}} = -h_{t+1} A_t^{-1} (\bar{Q}_{\text{Null}^\perp} \tilde{R}_{C,t} \bar{Q}_{\text{Null}}) W_t^{-1}, \quad b_{t+1} = u^T \Sigma_{t+1} \bar{Q} = C_{t+1} (b_t + R_{b,t}),$$

for $u = g/\|g\|$ the normalized gradient vector. In the first term, the product $(\bar{Q}_{\text{Null}^\perp} \tilde{R}_{C,t} \bar{Q}_{\text{Null}}) W_t^{-1} = \Theta(1)$, hence the rate is dominated by the second order anisotropy $h_{t+1} A_t^{-1} = \Theta(\sqrt{h_t})$. For the final vector, $\|b_t + R_{b,t}\| = O(\|\Sigma_{\text{Null}^\perp}\|)$, hence we can combine this with our previous analysis to yield

$$\bar{Q}_{\text{Null}} C_{t+1} (b_t + R_{b,t}) = \Theta(1) O(\sqrt{h_t}) = O(\sqrt{h_{t+1}}), \quad \bar{Q}_{\text{Null}^\perp} C_{t+1} (b_t + R_{b,t}) = \Theta(h_{t+1}) O(\sqrt{h_t}) = O(h_{t+1}).$$

Note that the scalar inflation to go from h_t to h_{t+1} does not aggregate across iterations as the initial bound was driven by the second order anisotropy term, to which the remainders only contribute negligibly. \square

This verifies the claim for the recurrence in $\mathcal{L}(\mu_\zeta)$. Our goal now is to lift this analysis to $\mathcal{L}(\mu)$ with covariance cap ζ . The distinction between these recurrences is that the first a priori filters the Null direction out of the dynamics, whereas the latter trims any eigenvalues above a set threshold ζ . These recurrences coincide if the Null \times Null component never falls below the threshold ζ , thus we seek to identify such a threshold.

Proof of Theorem 3. Lemma 28 verifies the specified dynamics, particularly the Null \times Null component of $\Sigma_{i,\zeta}$ remains $\Theta(1)$, and thus there is some floor $\gamma(\zeta)$ which it never drops below. We now will argue that $\gamma(\zeta) > 0$ as $\zeta \rightarrow 0$, hence there exists a threshold ζ^* such that the filtered and cap dynamics coincide.

As $\zeta \rightarrow 0$, $H_\zeta \rightarrow H$, as the distribution concentrates about x^* , and in particular, for ζ small enough, the signature of H_ζ is the same as that of H . This follows from the maximal rank assumption on H . By Propositions 2 and 3, upon transforming

$C_{t,\zeta} \mapsto \frac{W_{\zeta}^T C_{t,\zeta} W_{\zeta}}{\sqrt{c(r,\beta)h_t}} =: X_{t,\zeta}$, $W_{\zeta} := U_{\zeta} |\Lambda_{\zeta}|^{1/2}$, for the diagonalization $H_{\zeta} = U_{\zeta} \Lambda_{\zeta} U_{\zeta}^T$, these recurrences are reduced to the same canonical form, with seeds depending smoothly on ζ . Applying Lemma 21, it follows that $X_{t,\zeta} = X_{t,0} + O(\zeta + \alpha)$.

Inverting the transformation, this yields $C_{t,\zeta} = C_{t,0} + O(\sqrt{h_t}(\delta + \alpha))$. Returning to the proof of Lemma 28,

$$\Sigma_{t,\text{Null},\zeta} = h_{t+1} (\bar{Q}_{\text{Null}} \tilde{R}_{C,t,\zeta} (\Sigma_{t,\text{Null}^{\perp},\zeta} \bar{Q}_{\text{Null}})^{-1} + O(\sqrt{h_t})) = \Sigma_{t,\text{Null}^{\perp},0} + O(\sqrt{h_t}(\zeta + \alpha)),$$

hence for ζ, α sufficiently small the noise floor is non-vanishing as desired.

Thus the rates of Lemma 28 is achieved. Plugging these rates into our risk bounds yields $\sqrt{\det \Sigma_t} = \Theta(h_t^{(2d+1)/4})$, $W(\mu_t) = O(h_t)$, thus yielding the desired rate. \square

C. EGOP Approximation

In this section, we show that metric anisotropy not only improves point regression, but accelerates the estimation of the EGOP matrix in our two model settings. We argue that the smoothed gradients, while potentially biased estimators at individual points, in the aggregate form a matrix that differs from the population quantity by a benign perturbation, leading to an equivalent convergence analysis at adequate sample sizes.

Define the smoothed gradient and EGOP as

$$\nabla_{\Sigma} f(x) = \operatorname{argmin}_v \min_a \int \|f(z) - a - v(z - x)\|^2 dN(x, \Sigma), \quad \mathcal{L}_{\Sigma}(\mu) = \int \nabla_{\Sigma} f \nabla_{\Sigma} f^T d\mu.$$

We study the covariance recurrence

$$\Sigma_{t+1} = h_{t+1} [\beta \hat{\mathcal{L}}_{\Sigma_t}(\mu_t) + (1 - \beta) \hat{\mathcal{L}}_{\Sigma_{t-1}}(\mu_{t-1})]^{-1} =: h_{t+1} [\hat{M}_t]^{-1}. \quad (9)$$

Lemma 29 (Smoothed Gradient). *There exists T_x, C , $T_x(\Sigma) \leq C\|\Sigma\|$ such that, for $\mu = N(x^*, \Sigma)$,*

$$\nabla_{\Sigma} f = \nabla f + T_x(\Sigma), \quad \mathcal{L}_{\Sigma}(\mu) = \mathcal{L}(\mu) + \mathbb{E}_{\mu}[g T_X(\Sigma)^T + T_X(\Sigma) g^T] + O(\|\Sigma\|^2).$$

Proof. The standard OLS solution yields

$$\nabla_{\Sigma} f(x) = \Sigma^{-1} \operatorname{Cov}_{N(x, \Sigma)}(X, f(X)) = \mathbb{E}_{N(x, \Sigma)}[\nabla f(X)],$$

with the last equality following from Stein's Identity (Stein, 1981). Applying a Taylor expansion, we see that

$$\mathbb{E}_{N(x, \Sigma)}[\nabla f(X)] = \int \nabla f(x) + H(y - x) + T_x(y - x, y - x) dN(0, \Sigma) =: \nabla f(x) + T_x(\Sigma),$$

where T_x is a second order remainder. For the second claim, the proof follows by a simple expansion,

$$\begin{aligned} \mathcal{L}_{\Sigma}(\mu) &= \int \nabla_{\Sigma} f \nabla_{\Sigma} f^T d\mu \\ &= \int \nabla f \nabla f^T d\mu + \int T_x(\Sigma) \nabla f^T + \nabla f T_x(\Sigma) d\mu \\ &= \mathcal{L}(\mu) + \int T_x(\Sigma) g^T + g T_x(\Sigma) d\mu + \int T_x(\Sigma) (\nabla f - g)^T + (\nabla f - g) T_x(\Sigma) d\mu, \end{aligned}$$

satisfying the claim, with full details being similar to those in the proof of Lemma 3. \square

This expansion is satisfactory for the full-rank setting, indeed, one can substitute \mathcal{L}_{Σ} into the recurrence of Equation 2, and arrive at the same expansion of Lemma 3. A more refined expansion is necessary for the continuous index setting. Let Null_x denote the null subspace at point x .

Lemma 30. (Anisotropic Smoothed Gradient) *Let (X, Y) satisfy the supervised noisy manifold hypothesis, $D > 2d$. There exists $T_{x,\Sigma_{\text{Null}_x}}$ and a uniform constant C satisfying $T_{x,\Sigma_{\text{Null}_x}}(A) \leq C\|A\|$, such that*

$$\nabla_{\Sigma} f(x) = \nabla f(x) + T_{x,\Sigma_{\text{Null}_x}}(\Sigma_{\text{Null}_x^{\perp}} - [\pi_{\text{Null}_x^{\perp}} \Sigma \pi_{\text{Null}_x}] \Sigma_{\text{Null}_x}^{-1} [\pi_{\text{Null}_x} \Sigma \pi_{\text{Null}_x^{\perp}}])$$

Proof. We combine Stein's identity with Lemma 1 to yield

$$\begin{aligned}
 \nabla_{\Sigma} f(x) &= \mathbb{E}_{N(x, \Sigma)} [\nabla f(X)] = \int \nabla f(y) dN(y; x, \Sigma) \\
 &= \int \left(\int \nabla f(y) d\mu_v \right) d\nu(v) = \nabla f(x) + \int T_v(\Sigma_v) d\nu(v) \\
 &=: \nabla f(x) + T_{x, \Sigma_{\text{Null}_x}} (\Sigma_{\text{Null}_x^\perp} - [\pi_{\text{Null}_x^\perp} \Sigma \pi_{\text{Null}_x}] \Sigma_{\text{Null}_x}^{-1} [\pi_{\text{Null}_x} \Sigma \pi_{\text{Null}_x^\perp}]).
 \end{aligned}$$

□

Lemma 31 (Anisotropic Rotation). *For x within a neighborhood of x^* ,*

$$\begin{aligned}
 \|\pi_{\text{Null}_x^\perp} \Sigma \pi_{\text{Null}_x}\| &= O(\|\pi_{\text{Null}_{x^*}^\perp} [x - x^*]\| + \|\pi_{\text{Null}^\perp} \Sigma \pi_{\text{Null}}\|), \quad \|\Sigma_{\text{Null}_x^\perp}^{-1}\| \leq 2/\lambda_{\min}(\Sigma_{\text{Null}^\perp}), \\
 \|\Sigma_{\text{Null}_x^\perp}\| &= O(\|\pi_{\text{Null}_{x^*}^\perp} [x - x^*]\|^2 + \|\Sigma_{\text{Null}^\perp}\| + \|\pi_{\text{Null}_{x^*}^\perp} [x - x^*]\| \|\Sigma \pi_{\text{Null}^\perp}\|).
 \end{aligned}$$

Proof. We first show that

$$\|\pi_{\text{Null}_x} - \pi_{\text{Null}_{x^*}}\| = O(\pi_{\text{Null}_{x^*}^\perp} [x - x^*]),$$

from which the desired result follows easily. As characterized in the proof of Lemma 5, $\text{Null}_x = \phi_{\pi(x), \nabla f(x)}(\mathcal{T}_x)^\perp$, for $\phi_{\pi(x), u}(w) := \mathbb{I}_{\pi(x)}(u, w)$. Thus we see that this subspace changes smoothly in the displacement of the basepoint $\pi(x)$ or the gradient $\nabla f(x)$, i.e. along Null_x^\perp .

Thus, setting $D_x := \pi_{\text{Null}_x^\perp} - \pi_{\text{Null}_{x^*}^\perp}$,

$$\begin{aligned}
 \|\pi_{\text{Null}_x^\perp} \Sigma \pi_{\text{Null}_x}\| &= \|(\pi_{\text{Null}_{x^*}^\perp} + D_x) \Sigma (\pi_{\text{Null}_{x^*}} - D_x)\| \\
 &\leq \|\pi_{\text{Null}^\perp} \Sigma \pi_{\text{Null}}\| + C\|D_x\| + C'\|D_x\|^2 \\
 &= O(\|\pi_{\text{Null}^\perp} \Sigma \pi_{\text{Null}}\| + \|\pi_{\text{Null}_{x^*}^\perp} [x - x^*]\|),
 \end{aligned}$$

as desired. The third claim follows in the exact same way, stopping at the second line of the derivation. The second claim follows by continuity. □

It is again necessary to localize and extend f so that these constraints are globally active, or contract the covariance cap $\zeta_t \rightarrow 0$ at a logarithmic rate.

Lemma 32 (Anisotropic Gradient Bound). *Let (X, Y) satisfy the supervised noisy manifold hypothesis, $D > 2d$. There exists $T_{x, \Sigma_{\text{Null}_x}}$ and a uniform constant C satisfying $T_{x, \Sigma_{\text{Null}_x}}(A) \leq C\|A\|$, such that*

$$\nabla_{\Sigma} f(x) = \nabla f(x) + T_{x, \Sigma_{\text{Null}_x}} (\Sigma_{\text{Null}^\perp}) + R(x),$$

for $R(x) = O(\|\pi_{\text{Null}^\perp} [x - x^*]\|^2 + \|\pi_{\text{Null}^\perp} [x - x^*]\| \|\pi_{\text{Null}^\perp} \Sigma\| + \|\pi_{\text{Null}^\perp} \Sigma\|^2 + \|\Sigma_{\text{Null}^\perp}\|)$.

Proof. By Lemma 30 we can express

$$\begin{aligned}
 \nabla_{\Sigma} f(x) &= \nabla f(x) + T_{x, \Sigma_{\text{Null}_x}} (\Sigma_{\text{Null}_x^\perp} - [\pi_{\text{Null}_x^\perp} \Sigma \pi_{\text{Null}_x}] \Sigma_{\text{Null}_x}^{-1} [\pi_{\text{Null}_x} \Sigma \pi_{\text{Null}_x^\perp}]) \\
 &=: \nabla f(x) + T_{x, \Sigma_{\text{Null}_x}} (\Sigma_{\text{Null}^\perp}) + R(x).
 \end{aligned}$$

That $R(x)$ satisfies the appropriate bound is an immediate consequence Lemma 31 and the Lipschitz continuity of T . □

Lemma 33 (Anisotropic Smoothed EGOP). *Let (X, Y) satisfy the supervised noisy manifold hypothesis, $D > 2d$. Then*

$$\mathcal{L}_{\Sigma}(\mu) = \mathcal{L}(\mu) + \mathbb{E}_{\mu} [g T_{X, \Sigma_{\text{Null}_X}} (\Sigma_{\text{Null}^\perp})^T + T_{X, \Sigma_{\text{Null}_X}} (\Sigma_{\text{Null}^\perp}) g^T] + R(\Sigma),$$

for

$$R(\Sigma) = O(\|\Sigma_{\text{Null}^\perp}\| + \|\pi_{\text{Null}^\perp} \Sigma\|^2 + \sqrt{\|\Sigma_{\text{Null}^\perp}\|} \|\pi_{\text{Null}^\perp} \Sigma\|).$$

Proof. This result is an immediate consequence of Lemma 32 in combination with Isserlis's Theorem (Isserlis, 1918), see Lemma 3 for a similar computation. □

Thus we have achieved a remainder control that is tight under anisotropy, where Σ may stretch in the Null direction without severe consequence. Our primary assumption will be regarding the accuracy of gradient estimation.

Lemma 34 (EGOP Approximation). *Suppose that $\|\nabla_{\Sigma} \hat{f} - \nabla_{\Sigma} f\|_{L^2(\mu)} = O(n^{-1} \det(\Sigma_t^{-1/2}))$. Then,*

$$\hat{\mathcal{L}}_{\Sigma}(\mu) = \mathcal{L}_{\Sigma}(\mu) + O\left(\frac{1}{n\sqrt{\det(\Sigma_t)}}\right).$$

Proof. We compute,

$$\begin{aligned} \|\hat{\mathcal{L}}_{\Sigma}(\mu) - \mathcal{L}_{\Sigma}(\mu)\| &= \left\| \int \nabla_{\Sigma} \hat{f} \nabla_{\Sigma} \hat{f}^T - \nabla_{\Sigma} f \nabla_{\Sigma} f^T \, d\mu \right\| \\ &\leq \int \|\nabla_{\Sigma} \hat{f} - \nabla_{\Sigma} f\| \|\nabla_{\Sigma} f\| + \|\nabla_{\Sigma} \hat{f} - \nabla_{\Sigma} f\| \|\nabla_{\Sigma} \hat{f}\| \, d\mu \\ &= O\left(\frac{1}{n\sqrt{\det(\Sigma_t)}}\right). \end{aligned}$$

□

We note that the indicated rate is typical when utilizing standard nonparametric estimators, such as via local linear regression, and can be achieved by taking the covariance cap $\zeta \rightarrow 0$ at an appropriate rate. This condition is less easily satisfied for fully anisotropic Σ_t .

Proposition 4 (Full Rank Empirical Guarantee). *Let H be full rank, and suppose that $\|\nabla_{\Sigma_t} \hat{f} - \nabla_{\Sigma_t} f\|_{L^2(\mu_t)} \leq Cn^{-1} \det(\Sigma_t^{-1/2})$. Adopt the assumptions of Theorem 1. Then, for Σ_t satisfying Equation 9, for $t_n = \frac{4 \log n}{(D+5) \log(1/r)}$,*

$$\mathbb{E} \left[\int (\hat{P}_{\hat{M}_{t_n}}(f) - f)^2 \, d\mu_{t_n} \right] = O\left(n^{-\frac{4}{D+5}}\right).$$

Proof. By Lemma 29 we see that $\hat{\mathcal{L}}(\mu)$ satisfies an equivalent expansion to Lemma 3 up to $O(n^{-1} \det(\Sigma_t^{-1/2}))$ approximation error. As argued in the proof of Theorem 1, the second order recurrence is asymptotically autonomous so long as the empirical error is negligible, satisfying $n^{-1} \det(\Sigma_t^{-1/2}) = O(h_t)$. Evaluating,

$$n^{-1} \det(\Sigma_{t_n}^{-1/2}) = n^{-1} h_{t_n}^{-(d+1)/4} = O(h_{t_n}).$$

□

Proposition 5 (Continuous Index Empirical Guarantee). *Let (X, Y) satisfy the supervised noisy manifold hypothesis, and $\text{rank}(H) = 2d$. Suppose that $\|\nabla_{\Sigma_t} \hat{f} - \nabla_{\Sigma_t} f\|_{L^2(\mu_t)} \leq Cn^{-1} \det(\Sigma_t^{-1/2})$. Adopt the assumptions of Theorem 3. Then, for the recurrence*

$$\Sigma_t = h_{t+1} [\beta \hat{\mathcal{L}}_{\Sigma}(\mu_t) + (1 - \beta) \hat{\mathcal{L}}_{\Sigma}(\mu_{t-1})]^{-1},$$

selecting $t_n = \frac{4 \log n}{(2d+5) \log(1/r)}$,

$$\mathbb{E} \left[\int (\hat{P}_{\hat{M}_{t_n}}(f) - f)^2 \, d\mu_{t_n} \right] = O\left(n^{-\frac{4}{2d+5}}\right).$$

Proof. The proof again follows immediately from our previous analysis, exploiting the robustness to perturbations we already verified. First however, we must verify that the expansions of Lemma 33 and Lemma 26 are equivalent, i.e. we must verify that

$$\|\pi_{\text{Null}^\perp} \Sigma_t\|^2, \sqrt{\|\Sigma_{t,\text{Null}^\perp}\|} \|\pi_{\text{Null}^\perp} \Sigma_t\| = O(\|\Sigma_{t,\text{Null}^\perp}\|), \quad (10)$$

along the smoothed recurrence. We do this first neglecting noise. The base case is the same, and we adopt the inductive hypothesis in the proof of Theorem 3. Condition (10) is weaker than this inductive hypothesis, and the remainder of the

argument is identical. Thus, it suffices to check that empirical error is negligible, satisfying $n^{-1} \det(\Sigma_t^{-1/2}) = O(h_t)$. Evaluating,

$$n^{-1} \det(\Sigma_t^{-1/2}) = n^{-1} h_{t_n}^{-(2d+1)/4} = O(h_{t_n}).$$

□

C.1. Additional Settings of Interest

Example 5 (Spheres). Built into Theorem 3 are assumptions on the ambient dimension and derivatives of f . The sphere S^{D-1} is a typical toy example, however $D \geq 2(D-1)$ fails for $D \geq 3$. In these settings, the hessian has the form

$$H = \begin{bmatrix} T & b \\ b^T & 0 \end{bmatrix}$$

in the $\mathcal{T} \times \mathcal{N}$ basis. Thus the noisy manifold hypothesis only guarantees that a single entry of the Hessian is 0. Hence, $\pi_{g^\perp} H \pi_{g^\perp}$ is generically full rank, driving second order anisotropy along the tangent and orthogonal, as demonstrated in Figure 8.

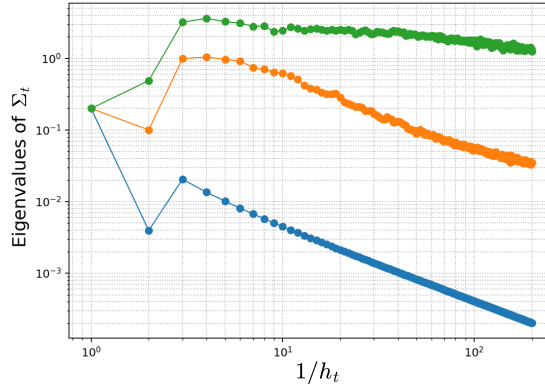


Figure 8. Eigenvalue decay of Σ_t with Local EGOP Learning applied to data satisfying the noisy manifold hypothesis about S^2 . The orthogonal exhibits light decay, approaching second order anisotropy asymptotically.